



## 7-Amino-[1,2,4]triazolo[1,5-a][1,3,5]triazines as CK1 $\delta$ inhibitors: Exploring substitutions at the 2 and 5-positions

Ilenia Grieco<sup>a</sup>, Davide Bassani<sup>b</sup>, Letizia Trevisan<sup>a</sup>, Veronica Salmaso<sup>b</sup>, Eleonora Cescon<sup>a</sup>, Filippo Prencipe<sup>a</sup>, Tatiana Da Ros<sup>a</sup>, Loreto Martinez-Gonzalez<sup>c,d</sup>, Ana Martinez<sup>c,d</sup>, Giampiero Spalluto<sup>a</sup>, Stefano Moro<sup>b</sup>, Stephanie Federico<sup>a,\*</sup>

<sup>a</sup> Dipartimento di Scienze Chimiche e Farmaceutiche, Università degli Studi di Trieste, Via Licio Giorgieri 1, 34127 Trieste, Italy

<sup>b</sup> Molecular Modeling Section (MMS), Dipartimento di Scienze del Farmaco, Università di Padova, via Marzolo 5, 35131 Padova, Italy

<sup>c</sup> Centro de Investigaciones Biológicas, CSIC, Avenida Ramiro de Maeztu 9, 28040 Madrid, Spain

<sup>d</sup> Centro de investigación biomédica en red en enfermedades neurodegenerativas (CIBERNED), Instituto de Salud Carlos III, Spain

### ARTICLE INFO

In memory of Silvia Dei

#### Keywords:

CK1  
CK1 $\delta$   
Protein kinase inhibitors  
ATP-competitive inhibitors  
[1,2,4]triazolo[1,5-a][1,3,5]triazines  
Neuroprotection  
Neurodegenerative diseases  
Amyotrophic Lateral Sclerosis  
TDP-43  
Parkinson's disease

### ABSTRACT

CK1 $\delta$  is a serine-threonine kinase involved in several pathological conditions including neuroinflammation and neurodegenerative disorders like Alzheimer's disease, Parkinson's disease, and Amyotrophic Lateral Sclerosis. Specifically, it seems that an inhibition of CK1 $\delta$  could have a neuroprotective effect in these conditions. Here, a series of [1,2,4]triazolo[1,5-a][1,3,5]triazines were developed as ATP-competitive CK1 $\delta$  inhibitors. Both positions 2 and 5 have been explored leading to a total of ten compounds exhibiting IC<sub>50</sub>s comprised between 29.1  $\mu$ M and 2.08  $\mu$ M. Three of the four most potent compounds (IC<sub>50</sub> < 3  $\mu$ M) bear a thiophene ring at the 2 position. All compounds have been submitted to computational studies that identified the chain composed of at least 2 atoms (e.g., nitrogen and carbon atoms) at the 5 position as crucial to determine a key bidentate hydrogen bond with Leu85 of CK1 $\delta$ . Most potent compounds have been tested *in vitro*, resulting passively permeable to the blood-brain barrier and, safe and slight neuroprotective on a neuronal cell model. These results encourage to further structural optimize the series to obtain more potent CK1 $\delta$  inhibitors as possible neuroprotective agents to be tested on models of the above-mentioned neurodegenerative diseases.

### 1. Introduction

Casein kinase 1 is a family of serine-threonine kinases that includes casein kinase 1 $\delta$  (CK1 $\delta$ ) and six other isoforms which are ubiquitously expressed and are involved in a plenty of signaling pathways [1]. Dysregulation of CK1 $\delta$  can lead to the occurrence of several pathological conditions including cancer [2–4], circadian rhythm disorders [5], infections [6,7] as well as neurodegenerative disorders [8]. Among neurodegenerative diseases, CK1 $\delta$  is implicated in Alzheimer's disease [9,10], Amyotrophic Lateral Sclerosis (ALS) [11] and Parkinson's disease [12], and all of these ailments share the presence of hyperphosphorylated and mislocalized proteins:  $\tau$  protein [10], transactive response DNA-binding protein 43 kDa (TDP-43) [13], and  $\alpha$ -synuclein [12], respectively. For these reasons, development of CK1 $\delta$  inhibitors is

crucial to validate the kinase as a reliable therapeutic target in the above-mentioned conditions. Most representative CK1 $\delta$  inhibitors reported in literature are shown in Fig. 1. The 1H-imidazole PF-670462 (I) is a well-recognized pharmacological tool for CK1 $\delta/\epsilon$  investigations, it shows an IC<sub>50</sub> value towards isoform  $\delta$  of 14 nM. For example, it has been used in studies concerning memory deficits, AD, and circadian rhythm disorders [14–16]. Pfizer has further explored the development of more potent inhibitors moving to pyrazole derivatives, including compound II which has an IC<sub>50</sub> of 6 nM and proved to be more selective towards isoform  $\delta$  compared to other kinases [17]. Among purines, SR-2890 (III) has revealed an IC<sub>50</sub> of 4 nM [18] and (R)-DRF053 (IV), developed by Oumat *et al.* as a Roscovitine-like compound, has reported a comparable potency in the low nanomolar range (14 nM) [19]. Another explored nucleus is the benzo[d]thiazole, where IGS2.7 (V)

\* Corresponding author.

E-mail addresses: [ilenia.grieco@phd.units.it](mailto:ilenia.grieco@phd.units.it) (I. Grieco), [davide.bassani.1@phd.unipd.it](mailto:davide.bassani.1@phd.unipd.it) (D. Bassani), [letizia.trevisan@phd.units.it](mailto:letizia.trevisan@phd.units.it) (L. Trevisan), [veronica.salmaso@unipd.it](mailto:veronica.salmaso@unipd.it) (V. Salmaso), [eleonora.cescon@phd.units.it](mailto:eleonora.cescon@phd.units.it) (E. Cescon), [filippo.prencipe@units.it](mailto:filippo.prencipe@units.it) (F. Prencipe), [daros@units.it](mailto:daros@units.it) (T. Da Ros), [loretomg@cib.csic.es](mailto:loretomg@cib.csic.es) (L. Martinez-Gonzalez), [ana.martinez@csic.es](mailto:ana.martinez@csic.es) (A. Martinez), [spalluto@units.it](mailto:spalluto@units.it) (G. Spalluto), [stefano.moro@unipd.it](mailto:stefano.moro@unipd.it) (S. Moro), [sfederico@units.it](mailto:sfederico@units.it) (S. Federico).

<https://doi.org/10.1016/j.bioorg.2024.107659>

Received 29 May 2024; Received in revised form 8 July 2024; Accepted 15 July 2024

Available online 17 July 2024

0045-2068/© 2024 The Author(s). Published by Elsevier Inc. This is an open access article under the CC BY license (<http://creativecommons.org/licenses/by/4.0/>).

with an  $IC_{50}$  of 23 nM has been investigated in ASL models [20,21].

The employment of [1,2,4]triazolo[1,5-*a*][1,3,5]triazine as scaffold for the development of series of ATP-competitive inhibitors has the advantage of mimicking the adenine core of ATP and offers the possibility to simultaneously investigate substitutions at the 2, 5 and 7-positions to find key structural features able to interact with the target kinase, CK1 $\delta$  (Fig. 2). Recently, our research group developed a series of [1,2,4]triazolo[1,5-*a*][1,3,5]triazine as CK1 $\delta$  inhibitors [22], where phenol-like substituents were present at the 2-position of the bicyclic nucleus and different benzylamines or cyclohexylamine were introduced at the 5-position. Position 7 was occupied by a free amino group able to interact with residues of the hinge region of CK1 $\delta$ . The preliminary investigation has led to the discovery of a hit compound (VI, Fig. 2) [22] but the structure–activity relationship (SAR) profile has not been thoroughly explored.

To fully investigate 2 and 5-positions of the nucleus, in this work, the first goal is represented by the exploration of the 5-position without substituents at 2-location, followed by introducing contemporarily both aromatic and aliphatic substituents at the 2 position and different key amines at the 5-position (Fig. 2). Exploration of SAR of these series aims in the end to develop compounds that can represent a good starting point for the outcome of more potent inhibitors as potential agents for neurodegeneration treatment.

## 2. Results and discussion

### 2.1. Chemistry

The [1,2,4]triazolo[1,5-*a*][1,3,5]triazine derivatives (28–73) have been synthesized following the strategy and procedures of Caulkett *et al.* properly modified (Scheme 1) [23].

The synthesis started from the commercially available cyanuric chloride (1) that, by reaction with phenol under reflux, was converted into 2,4,6-triphenoxy-1,3,5-triazine (2). Two different pathways, A and B (Scheme 1), can be used to obtain the desired *N'*-(4,6-diphenoxy-1,3,5-triazin-2-yl)hydrazides (4–11). In pathway A, compound 2 was directly reacted with the corresponding hydrazides, while in pathway B, compound 2 was firstly monosubstituted with hydrazine to afford compound 3, and then, it reacted with the desired acyl chlorides or formic acid at *N'* position. In particular, pathway A has been used for aryl or methyl hydrazides and pathway B for cycloalkyl or unsubstituted hydrazides. In fact, reactions between 2,4,6-triphenoxy-1,3,5-triazine

(2) and cyclobutane or cyclopentane carboxylic acid hydrazides have been resulted in very low yields following pathway A. With compounds 4–11 in our hands, a dehydrative cyclization with phosphorous pentoxide and hexamethyl-disiloxane in anhydrous xylene was required to achieve 5,7-diphenoxy-[1,2,4]triazolo[1,5-*a*][1,3,5]triazines (12–19). The yields of intramolecular cyclization are strongly affected by the nature of substituent linked by hydrazide moiety: a marked difference has been experimentally detected with methoxyphenyl hydrazide in comparison to thienyl hydrazide that positively impacts yields of cyclization allowing to collect a great amount of final compounds. The next synthetic steps involved firstly the addition of methanolic ammonia to obtain 5-phenoxy-[1,2,4]triazolo[1,5-*a*][1,3,5]triazin-7-amines (20–27) and then a nucleophilic substitution with the desired amines performed in a sealed tube, using ethanol or butanol as solvents, to explore the substitution at the 5-position of the bicyclic scaffold (28–67). In some cases, *N*<sup>5</sup>,*N*<sup>7</sup>-bisamine derivatives were also obtained as by product of this last reaction. Some of that, compounds 68–73, were isolated and characterized to be then tested on CK1 $\delta$  [24–26].

### 2.2. Structure activity relationship studies

The developed derivatives 28–67 along with the 5,7-disubstituted compounds 68–73 have been firstly tested on CK1 $\delta$  at fixed concentration of 40  $\mu$ M using a luminescence-based assay, then  $IC_{50}$ s were determined only for compounds showing an inhibition of enzymatic activity percentage upper than 50 % at that concentration. All results are reported in Tables 1–2.

#### 2.2.1. Investigations at the 5-position

The first goal has been represented by the exploration of the substitutions at the 5 position without substituents at 2-location (Table 1).

Compound 74, already reported in the previous work, bears, as the hit compound VI, a simple benzylamine at this position, and, due to its ability to inhibit the activity of CK1 $\delta$  of 49.3 % when tested at the concentration of concentration of 40  $\mu$ M, could be considered as showing an  $IC_{50}$  about 40  $\mu$ M towards the target enzyme [27]. Thus, starting from compound 74, a series of derivatives (28–43,68–72) has been developed.

The activity has been improved considering phenylethylamine (42) as *R*<sup>1</sup> substituent achieving an optimizable  $IC_{50}$  of 29.1  $\mu$ M. The attempt to improve the molecule activity by introducing the pyridin-4-ylmethyl group instead of benzyl moiety (41) failed. Evaluating the possibility to

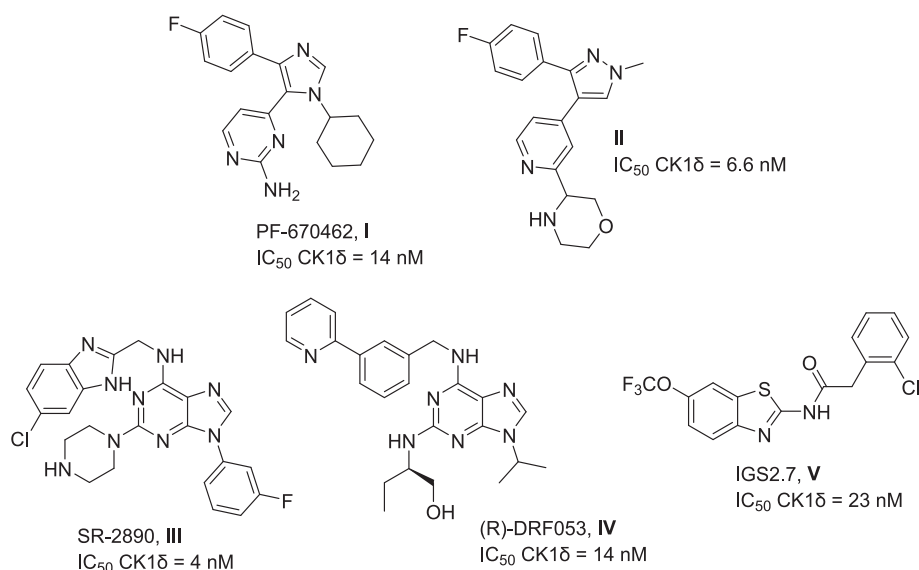
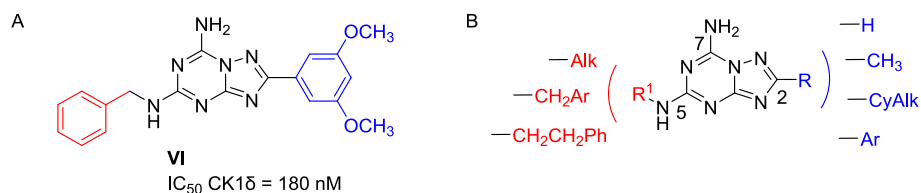
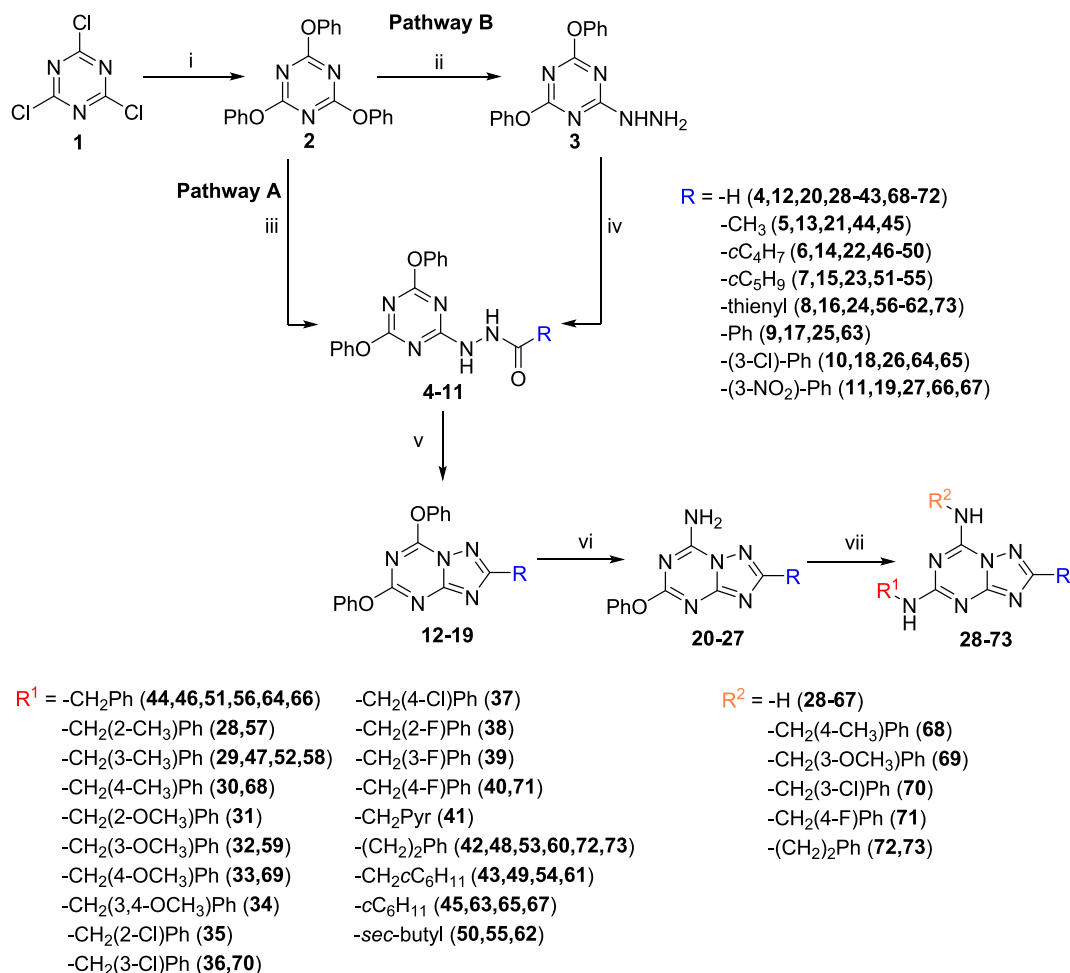


Fig. 1. Representative CK1 $\delta$  inhibitors.



**Fig. 2.** A) Previous developed CK1δ inhibitor with a [1,2,4]triazolo[1,5-*a*][1,3,5]triazine scaffold, compound VI; B) Chemical space investigated on [1,2,4]triazolo[1,5-*a*][1,3,5]triazine nucleus in this work.



**Scheme 1.** Synthesis of final compounds 28–73. Reagents and conditions: (i): PhOH, rfx; (ii): NH<sub>2</sub>NH<sub>2</sub>·H<sub>2</sub>O, DCM, r.t.; (iii): RCONHNH<sub>2</sub>, DBU, THF, r.t.; (iv): RCOCl or formic acid, DCM, TEA, 0 °C; (v): P<sub>2</sub>O<sub>5</sub>, HMDSO, anhydrous xylene, rfx; (vi): NH<sub>3</sub> in MeOH 7 N, r.t.; (vii): R<sup>1</sup>NH<sub>2</sub>, EtOH, 90–95 °C.

functionalize benzylamine at 2, 3 and 4 positions, several derivatives have been carried out. Starting from a simple methyl group, to methoxy group and halogens like chloride and fluorine have been inserted at the 2-position of benzylamine and all the developed compounds have proved to be not active towards CK1δ (28,31,35,38). The same rationale has been applied for the other positions: 3-methyl benzylamine derivative reported an IC<sub>50</sub> of 18.7 μM (29) and the activity improves by changing methyl moiety with chlorine atom, achieving an IC<sub>50</sub> of 9.26 μM (36). Curiously, the substitution of the same position with fluorine has led to the worsening of the activity (39). The high micromolar range has been maintained introducing 4-Cl-benzylamine group leading to an IC<sub>50</sub> of 23.8 μM (37) but trying to change chlorine atom with fluorine, methyl or methoxy moieties at the same position, compounds have been found to be inactive (40,30,33). Observing data for the same substitution at different positions becomes clear that a common behavior can be observed: with an increase of inhibitory activity passing from

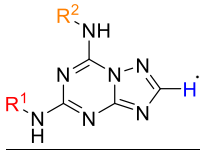
substitution at the 2 and 4 positions to the 3 position of the phenyl group (e.g. 2-substituted < 4-substituted < 3-substituted). For example, in chlorobenzyl subseries, 3-chlorobenzyl compound (36) exhibited an IC<sub>50</sub> of 9.26 μM, versus the 4-chlorobenzyl compound (37) that exhibited an IC<sub>50</sub> of 23.8 μM and the 2-chlorobenzyl compound (35) which resulted inactive at a concentration of 40 μM. Maintaining a comparable steric hindrance of benzyl moiety, cyclohexylmethyl has been inserted as R<sup>1</sup> at the 5-position improving the activity, achieving an IC<sub>50</sub> of 7.75 μM (43). Finally, all the N<sup>5</sup>-N<sup>7</sup> bis amine isolated derivatives 69–73, has led to inactive compounds, confirming our hypothesis that the free amino group at the 7 position is important to gain interactions with the enzyme residues, probably those belonging to the hinge region.

### 2.2.2. Investigations at the 2 position

To explore the 2 position, some key benzyl or alkyl moieties have been introduced on the amino group at the 5 position of the bicyclic

**Table 1**

Enzymatic inhibition activity of 2-unsubstituted[1,2,4]triazolo[1,5-*a*][1,3,5]triazine-5,7-diamine derivatives **28–43** and **68–72** on CK1δ



Cmpd	R <sup>1</sup>	R <sup>2</sup>	IC <sub>50</sub> <sup>a</sup> or % inhibition @40 μM
28	–CH <sub>2</sub> (2-CH <sub>3</sub> )Ph	–H	14.3 % ± 4.3 % <sup>b</sup>
29	–CH <sub>2</sub> (3-CH <sub>3</sub> )Ph	–H	18.7 μM ± 7.3 μM
30	–CH <sub>2</sub> (4-CH <sub>3</sub> )Ph	–H	43.9 % ± 21.9 % <sup>b</sup>
31	–CH <sub>2</sub> (2-OCH <sub>3</sub> )Ph	–H	20.2 % ± 15.9 % <sup>b</sup>
32	–CH <sub>2</sub> (3-OCH <sub>3</sub> )Ph	–H	43.6 % ± 9.0 % <sup>b</sup>
33	–CH <sub>2</sub> (4-OCH <sub>3</sub> )Ph	–H	31.8 % ± 9.1 % <sup>b</sup>
34	–CH <sub>2</sub> (3,4-OCH <sub>3</sub> )Ph	–H	42.8 % ± 10.3 % <sup>b</sup>
35	–CH <sub>2</sub> (2-Cl)Ph	–H	32.3 % ± 19.2 <sup>b</sup>
36	–CH <sub>2</sub> (3-Cl)Ph	–H	9.26 μM ± 2.64 μM
37	–CH <sub>2</sub> (4-Cl)Ph	–H	23.8 μM ± 5.2 μM
38	–CH <sub>2</sub> (2-F)Ph	–H	15.2 % ± 10.7 % <sup>c</sup>
39	–CH <sub>2</sub> (3-F)Ph	–H	43.2 % ± 6.8 % <sup>b</sup>
40	–CH <sub>2</sub> (4-F)Ph	–H	36.5 % ± 11.8 % <sup>b</sup>
41	–CH <sub>2</sub> (piridin-4-yl)	–H	22.8 % ± 17.1 % <sup>b</sup>
42	–(CH <sub>2</sub> ) <sub>2</sub> Ph	–H	29.1 μM ± 3.4 μM
43	–CH <sub>2</sub> (cC <sub>6</sub> H <sub>11</sub> )	–H	7.75 μM ± 1.96 μM
68	–CH <sub>2</sub> (4-CH <sub>3</sub> )Ph	–CH <sub>2</sub> (4-CH <sub>3</sub> )Ph	25.4 % ± 15.4 % <sup>b</sup>
69	–CH <sub>2</sub> (4-OCH <sub>3</sub> )Ph	–CH <sub>2</sub> (4-OCH <sub>3</sub> )Ph	12.2 % ± 21.8 % <sup>b</sup>
70	–CH <sub>2</sub> (3-Cl)Ph	–CH <sub>2</sub> (3-Cl)Ph	22.3 % ± 22.3 % <sup>b</sup>
71	–CH <sub>2</sub> (4-F)Ph	–CH <sub>2</sub> (4-F)Ph	15.9 % ± 14.3 % <sup>b</sup>
72	–(CH <sub>2</sub> ) <sub>2</sub> Ph	–(CH <sub>2</sub> ) <sub>2</sub> Ph	8.7 % ± 12.7 % <sup>b</sup>
74	–CH <sub>2</sub> Ph	–H	49.3 % <sup>d</sup>
I			10.5 nM ± 5.3 nM

<sup>a</sup> Data represent the mean ± SD of three independent experiments performed in technical duplicate.

<sup>b</sup> Data represent the % of CK1δ inhibition at 40 μM inhibitor concentration expressed as a mean ± SD of three independent experiments performed in technical duplicate.

<sup>c</sup> Data represent the % of CK1δ inhibition at 40 μM inhibitor concentration expressed as a mean ± SD of two independent experiments performed in technical duplicate.

<sup>d</sup> Compound previously reported in reference [27].

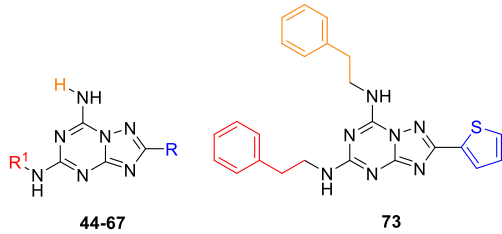
nucleus, comprised the promising cyclohexylmethyl moiety, that exhibited the best result among the 2-unsubstituted subseries (**28–43**). Then, three different alkyl substituents have been introduced at position 2, starting from a simple methyl group and increasing the steric hindrance introducing cyclic chains like cyclobutyl and cyclopentyl rings (**44–55**, Table 2). To explore aromatic substituents, phenyl ring has been inserted, followed by functionalized phenyl moieties as well as the heteroaromatic ring thiophene (**56–67**, Table 2).

Concerning aliphatic substitutions, 2-methyl derivatives proved to be not active with both benzylamine and cyclohexylamine at the 5 position (**44,45**); the attempts to increase the hindrance with bulkier substituents proved to be challenging. The introduction of the cyclobutyl moiety resulted in an IC<sub>50</sub> of 19.30 μM (**46**) and the activity has improved with cyclopentyl at the 2-position achieving an IC<sub>50</sub> of 2.91 μM (**51**), both the derivatives presented a benzylamine at the 5-position. Also, cyclohexylamino and branched *sec*-butylamino derivatives (**49,54** and **50,55**, respectively) have been developed but the IC<sub>50</sub>s have not been determined since they are not active towards the enzyme at a concentration of 40 μM, as reported in Table 2. Thus, starting from benzylamine at position 5 the length of the linker between the aryl ring and the scaffold have been increased by one methyl group, leading to a worsening of activity (**46** vs **53**), and the same result has been pointed out functionalizing benzylamine group with a methyl at 3-position for both the 2-cycloalkyl derivatives (**47,52**).

Few attempts have been carried out also with aromatic substituents at the 2-position; phenyl, even with a cyclohexylamino moiety at the 5-

**Table 2**

Enzymatic inhibition activity of 2-substituted[1,2,4]triazolo[1,5-*a*][1,3,5]triazine-5,7-diamine derivatives **44–67** and **73** on CK1δ



Cmpd	R	R <sup>1</sup>	IC <sub>50</sub> <sup>a</sup> or % inhibition @40 μM
44	–CH <sub>3</sub>	–CH <sub>2</sub> Ph	35.2 % ± 2.3 % <sup>b</sup>
45	–CH <sub>3</sub>	–(cC <sub>6</sub> H <sub>11</sub> )	33.8 % ± 22.1 % <sup>b</sup>
46	–cC <sub>4</sub> H <sub>7</sub>	–CH <sub>2</sub> Ph	19.3 μM ± 5.7 μM
47	–cC <sub>4</sub> H <sub>7</sub>	–CH <sub>2</sub> (3-CH <sub>3</sub> )Ph	11.5 % ± 16.8 % <sup>c</sup>
48	–cC <sub>4</sub> H <sub>7</sub>	–CH <sub>2</sub> CH <sub>2</sub> Ph	17.7 % ± 7.1 % <sup>c</sup>
49	–cC <sub>4</sub> H <sub>7</sub>	–CH <sub>2</sub> (cC <sub>6</sub> H <sub>11</sub> )	15.1 % ± 8.8 % <sup>c</sup>
50	–cC <sub>4</sub> H <sub>7</sub>	–CH(CH <sub>3</sub> )CH <sub>2</sub> CH <sub>3</sub>	9.7 % ± 7.6 % <sup>c</sup>
51	–cC <sub>5</sub> H <sub>9</sub>	–CH <sub>2</sub> Ph	2.91 μM ± 0.94 μM
52	–cC <sub>5</sub> H <sub>9</sub>	–CH <sub>2</sub> (3-CH <sub>3</sub> )Ph	27.8 % ± 21.5 % <sup>c</sup>
53	–cC <sub>5</sub> H <sub>9</sub>	–CH <sub>2</sub> CH <sub>2</sub> Ph	10.3 % ± 6.5 % <sup>c</sup>
54	–cC <sub>5</sub> H <sub>9</sub>	–CH <sub>2</sub> (cC <sub>6</sub> H <sub>11</sub> )	6.4 % ± 5.5 % <sup>c</sup>
55	–cC <sub>5</sub> H <sub>9</sub>	–CH(CH <sub>3</sub> )CH <sub>2</sub> CH <sub>3</sub>	8.2 % ± 4.6 % <sup>c</sup>
56	–2-thienyl	–CH <sub>2</sub> Ph	2.55 μM ± 0.78 μM
57	–2-thienyl	–CH <sub>2</sub> (2-CH <sub>3</sub> )Ph	2.08 μM ± 0.38 μM
58	–2-thienyl	–CH <sub>2</sub> (3-CH <sub>3</sub> )Ph	42.5 % ± 4.3 % <sup>c</sup>
59	–2-thienyl	–CH <sub>2</sub> (3-OCH <sub>3</sub> )Ph	2.74 μM ± 0.76 μM
60	–2-thienyl	–CH <sub>2</sub> CH <sub>2</sub> Ph	25.7 % ± 10.1 % <sup>c</sup>
61	–2-thienyl	–CH <sub>2</sub> (cC <sub>6</sub> H <sub>11</sub> )	45.3 % ± 20.8 % <sup>c</sup>
62	–2-thienyl	–CH(CH <sub>3</sub> )CH <sub>2</sub> CH <sub>3</sub>	38.7 % ± 5.9 % <sup>b</sup>
63	–Ph	–(cC <sub>6</sub> H <sub>11</sub> )	24.5 % ± 21.4 % <sup>c</sup>
64	–(3-Cl)Ph	–CH <sub>2</sub> Ph	15.2 % ± 7.0 % <sup>b</sup>
65	–(3-Cl)Ph	–(cC <sub>6</sub> H <sub>11</sub> )	1.1 % ± 14.5 % <sup>b</sup>
66	–(3-NO <sub>2</sub> )Ph	–CH <sub>2</sub> Ph	34.6 % ± 27.0 % <sup>b</sup>
67	–(3-NO <sub>2</sub> )Ph	–(cC <sub>6</sub> H <sub>11</sub> )	10.7 % ± 10.3 % <sup>b</sup>
73	–2-thienyl	–CH <sub>2</sub> CH <sub>2</sub> Ph	6.5 % ± 17.2 % <sup>c</sup>
I			10.5 nM ± 5.3 nM <sup>b</sup>

<sup>a</sup> Data represent the mean ± SD of three independent experiments performed in technical duplicate.

<sup>b</sup> Data represent the % of CK1δ inhibition at 40 μM inhibitor concentration expressed as a mean ± SD of two independent experiments performed in technical duplicate.

<sup>c</sup> Data represent the % of CK1δ inhibition at 40 μM inhibitor concentration expressed as a mean ± SD of three independent experiments performed in technical duplicate.

position have not provided to give an active derivative (**63**), and the same for 3-substituted phenyl rings with chlorine or nitro groups (**64–67**) that turned out to be inactive at a fixed concentration of 40 μM. Finally, five-membered aromatic heterocycle thiophene has been introduced at the 2-position, and, when benzylamine have been maintained at the 5 position, the developed derivative **56** shown the best IC<sub>50</sub> of the series, with a value of 2.55 μM. Unfortunately, after the substitution with the other moieties already investigated for the other radicals at the 2 positions, compounds **58,60–62** a detrimental effect on activity towards CK1δ has been observed. But the SAR profile has been further investigated by synthesizing thien-2-yl derivatives studying other two substitutions at the 5-position trying to optimize the activity of compound **56** (IC<sub>50</sub> CK1δ = 2.55 μM). The 3-methoxy candidate **59** showed an IC<sub>50</sub> of 2.74 μM while the 2-methyl benzylamino compound **57** has reported an IC<sub>50</sub> of 2.08 μM, resulting other two promising compounds of the series.

The most promising compound, compound **57**, has been evaluated for its behavior in kinase inhibition. A Lineweaver-Burk plot has been built up and since no variation in V<sub>max</sub> has been noticed in absence (control experiment) and presence of different concentration of inhibitor, it is possible to state the ATP-competitive behavior of compound **57**, as reported in Fig. 3.

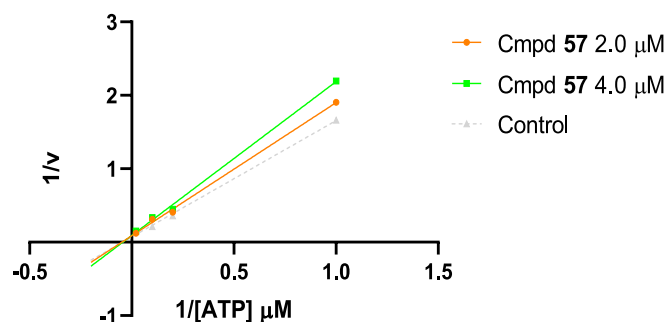


**Fig. 3.** Lineweaver-Burk plot for compound 57. The intercept with y-axis ( $V_{max}$ ) does not change in absence (control curve) or presence of the inhibitor confirming ATP-competitive behavior. The ATP-competition experiments have been performed in duplicate. Data used for analysis are reported in Table S4 using the calibration curves represented in Fig. S6.

### 2.3. Computational studies

To evaluate the interaction of the compounds synthesized and tested in the present study with the protein kinase CK1 $\delta$ , a computational study was executed. The specific workflow followed is deeply discussed in the Supporting Information, however we report here some main technical details for the *in silico* part of the work. Here we compare some selected poses coming from our strategy, based on docking and MD-based post-docking, to help rationalization of the obtained pharmacological results on the series (Figs. 4 and 5).

Specifically, Fig. 4 represents two of the most active compounds, 51 and 59 (respective potencies: 2.91  $\mu$ M and 2.74  $\mu$ M), while Fig. 5 depicts the binding modes of two molecules tested as inactive, 24 (see Table S1) and 65.

By the comparison of the compounds' docking poses is possible to point out some key factors. First, all the active compounds show the typical bidentate hydrogen bond with Leu85 (as shown in both the compounds of Fig. 4 and also in the panel B of Fig. 5), which is characteristic of CK1 $\delta$  ATP-competitive inhibitors. Compound 24 (Fig. 5, panel A), which has an oxygen atom replacing the nitrogen one (which is much more common in the series under evaluation), lacks in this type of favorable interaction. On the other hand, not just the final state of the molecule has to be considered, but also the path necessary for the ligand to approach the binding site. In this sense, having at position 5 of the triazolo-triazine scaffold a chain composed of at least 2 atoms (e.g., nitrogen and carbon atoms) might help the molecule to be correctly oriented in the binding pocket, placing the nitrogen atoms in the correct position to exploit better the interaction with the hinge region. The

presence of smaller chains in position 2, such as the one of 24, allows the molecule to explore a wider range of binding conformations with the catalytic site of the target, but, being the majority of these poses not proficient for the interaction, this could be the cause of an overall lowering in the potency of such ligands. Compound 65, on the other hand, shows an interaction pattern with the protein which is more similar to the one typical of the two aforementioned active compounds. Even if in this case could seem harder to rationalize from a structure-based perspective the reasons why the compound shows such a drop in activity, one point can be addressed to dynamic reasons. Indeed, the presence of a chlorophenyl group as the R substituent, which should place in the back of the pocket, makes harder for the compound to be allocated in the proposed binding mode, because of possible clashes during the entering process of the molecule in the pocket. Indeed, all the compounds of the 2-substituted[1,2,4]triazolo[1,5-a][1,3,5]triazine-5,7-diamine derivatives series which show biological activity have no more than five-member rings in the R position. To further evaluate such a recognition mechanism, one of the most appropriate techniques is Supervised Molecular Dynamics [28], also known as SuMD, which makes it possible to proficiently sample the steps performed by a ligand in approaching its binding site. This approach has already been validated on several different protein–ligand systems, as literature assesses [2930] The computational evaluation of the present database using SuMD is ongoing in our laboratory and will be the main focus of future scientific work.

Looking at the MD simulations, even if their application for screening purposes has been well established, with many different papers assessing its proficient usage for candidate prioritization [31–33] it seems not to be the case for the series of compounds under evaluation in the present work. Indeed, as represented in Fig. S3, the geometric parameters of the RMSD and RMSF do not allow a clear distinction between active and inactive compounds, being all the values similar to one another (with some noticeable exceptions, such as 45 and 28). The energetical measurements derived from the MD simulation are also less proficient for candidate prioritization. Indeed, while some inactive compounds (e.g., 64, 66, and 53 show a very good interaction with the target from both the electrostatic, the hydrophobic, and the MM/GBSA perspectives, some active molecules (e.g., 29,36, and 37) display a much worse profile in their dynamic interaction with CK1 $\delta$ . Compound 24, which was previously mentioned as a negative example in the docking studies, shows good geometrical parameters (RMSD and RMSF) during the MD simulations, but an overall scarce interaction energy with the target.

Looking into the detail, we reported in the Supplementary Materials a video representing one of the replicas of two different CK1 $\delta$  ligands. Specifically, Video S2 shows one of the MD simulations executed on 38 (which has been demonstrated to be inactive in the *in vitro* assays

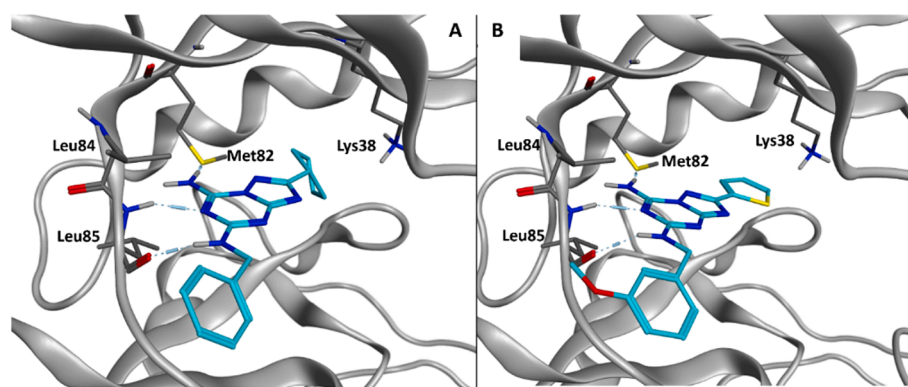


**Fig. 4.** Representation of the poses for the ligand 51 (panel A) and 59 (panel B) in the pocket of CK1 $\delta$  which were prioritized by our protocol. The small molecule inhibitors are colored in cyan, while the surrounding residues and the protein ribbons are colored in gray. The hydrogen bonds are depicted with dashed lines. The images were created and rendered with MOE. (For interpretation of the references to color in this figure legend, the reader is referred to the web version of this article.)



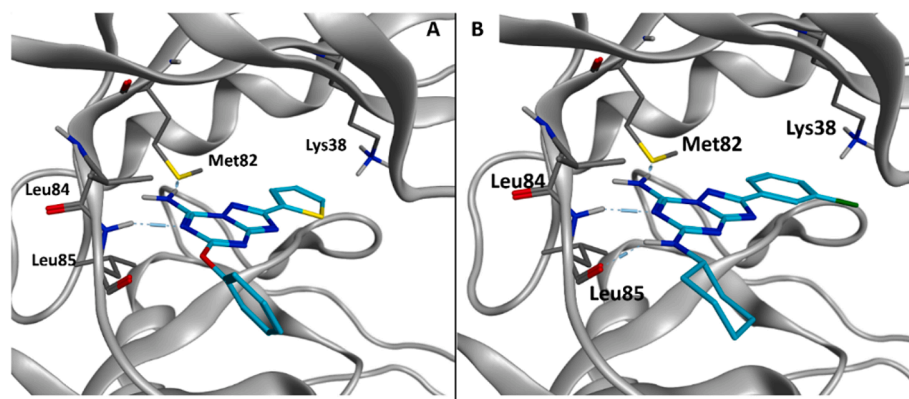


**Fig. 5.** Representation of the poses for the ligand **24** (panel A) and **65** (panel B) in the pocket of CK1 $\delta$  which were prioritized by our protocol. The small molecule inhibitors are colored in cyan, while the surrounding residues and the protein ribbons are colored in gray. The hydrogen bonds are depicted with dashed lines. The images were created and rendered with MOE. (For interpretation of the references to color in this figure legend, the reader is referred to the web version of this article.)

performed, represented on the left in the video) and one of the replicas of the molecule **51** (which has proven to be an effective CK1 $\delta$  inhibitor in the low micromolar range, on the right in the video). Because of the incoherency between the geometric and the energetic values coming from the post-docking refinement, was not considered an optimal example for the MD retrospective per-residue analysis, whereas **38** serve as a good case for this. The dynamic plots down reported in the video represent the overall per-residue interaction energy of the 25 residues which are the most contacted by the ligand during the trajectory. As depicted, a much more proficient interaction is retrievable for **51** rather than **38**, and this reflects also the difference reported in the plots in Fig. S3. This analysis demonstrates that relying on geometric parameters such as RMSD and RMSF can be very reductive in the description of ligand-target interaction from a molecular dynamics point of view, and for this reason, an in-depth analysis of the interaction energy should always be performed.

Also, in this case, the main limitation in the prioritization could be addressed to the fact that, even if MD examines the dynamic behavior of the compounds, the initial state provided in this case was the one coming from the docking run, as the method of MD-based post-docking requires. For this reason, all the molecular events derived from the approach of the ligand towards the target cannot be considered by this approach. We assess again that a more comprehensive vision of the reasons beneath the potency of the molecules of the present series will be obtained with the application of Supervised Molecular Dynamics, and the studies which are taking place in our lab will assess it.

#### 2.4. PAMPA: BBB permeability prediction assay

Since the therapeutic target of the work is the central nervous system (CNS), most promising compounds' capability to permeate the Blood Brain Barrier (BBB) was predicted by the PAMPA (Parallel Artificial Membrane Permeability Assay) – BBB assay.

The performed assay is based on an optimized protocol found in literature where Porcine Polar Brain Lipid (PBL) was used to mimic the composition of BBB cells. [34].

First, an evaluation of the linear correlation between literature and experimental data was performed, testing ten commercial drugs to determine *in vitro* permeability ( $P_e$ ) cut-offs that permits the classification of the inhibitor in permeable or not permeable (Table S3 and Fig. S5). In particular, compounds capable of penetrating the BBB (CNS+) are likely to have  $P_e$  value greater than  $4.0 \times 10^{-6}$  cm/s, on the other hand,  $P_e$  values of molecules that cannot pass through the membrane are usually lower than  $2.0 \times 10^{-6}$  cm/s [34]. The experimental  $P_e$  cut-off values determined for our experiment were  $2.14 \times 10^{-6}$  cm/s for

CNS+ and  $1.36 \times 10^{-6}$  cm/s for CNS-. Compounds having a  $P_e$  between these two values are in the zone of uncertainty and therefore were defined as borderline (CNS+/-). The three tested compounds result to be able to permeate through the BBB, as shown in Fig. 6A.

#### 2.5. Cell viability and neuroprotection assay

The assay consists in a reduction reaction of 3-(4,5-dimethylthiazol-2-yl)-2,5-diphenyltetrazolium bromide (MTT) to a formazan by enzymes metabolically active, during which a color change from yellow to purple occurs. Thank to this chromatic variation is possible to measure the solution absorbance at 500–600 nm to determine the number of active cells (the color intensity is related to the number of metabolically active cells, so the darker the solution the higher is the number of active cells [35]).

The most active compounds **56**, **57**, **59** have been chosen for this study. Human neuroblastoma SH-SY5Y cells were used as neuronal cell model and were incubated with compounds **56**, **57** and **59** for 24 h, to evaluate their toxicity on cells. Cell viability was calculated by comparison with non-treated cells. The first evaluation was made testing the compounds at  $5 \mu\text{M}$ , and all the compounds proved to be not toxic since the % cell viability is almost 100 %. Consequently, compounds were tested also at the higher concentration of  $10 \mu\text{M}$  and even in this case cells viability was always greater than 95 %, as represented in Fig. 6B. Thus, we can consider these compounds as not toxic for the specific cell line tested.

Since CK1 $\delta$  is involved in several neurodegenerative disorders, a possible neuroprotective behavior from our inhibitors was studied. In the neuronal cell model of human neuroblastoma SH-SY5Y cells, TDP-43 phosphorylation, which is pointed out to be one of the main hallmarks of ALS, was induced by ethacrynic acid (EA) treatment. A neuroprotective action on these cells should decrease the level of phosphorylated TDP-43 [36]. SH-SY5Y cells were preincubated with compounds **56**, **57** and **59** ( $5 \mu\text{M}$  concentration for all) and then treated with  $45 \mu\text{M}$  EA. After 24 h the MTT treatment allowed to measure the cell viability and, as shown in Fig. 6C, it resulted significantly decreased after the addition of EA (full black in the graph). Among the tested compounds, compounds **56** and **57** demonstrated a slight neuroprotection, comparing the cell viability with the cells treated only with EA. This effect is comparable with their low potency against the target CK1 $\delta$  and this is very promising for a future development of the series. In fact, a further structural optimization of the series to gain nanomolar inhibitory activities against kinase could lead to more potent neuroprotective agents. It is important to note that selectivity among kinases and, in particular, among different isoforms of the same family is an issue in the drug discovery of kinase

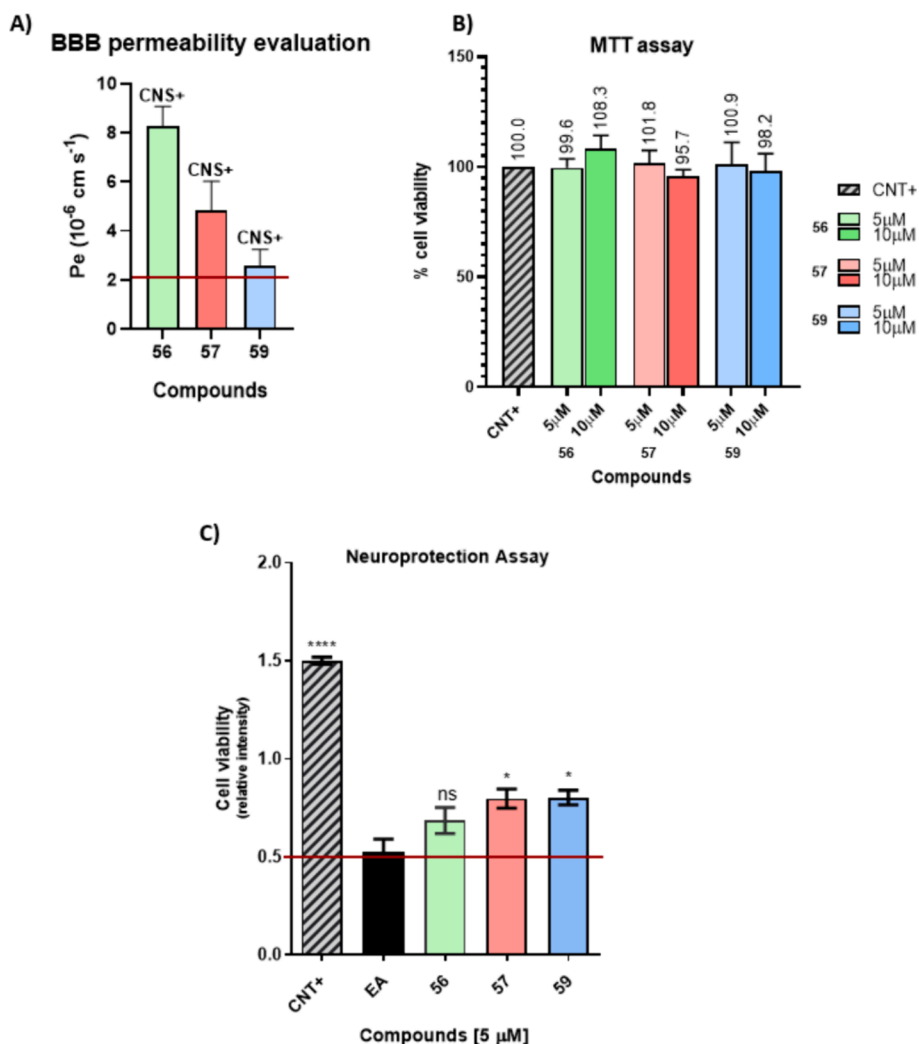


**Fig. 6.** Characterization of compounds 56, 57 and 59 for their use in neurodegenerative disorders. Panel A) BBB penetration prediction and classification based on PAMPA-BBB assay. The red line is the  $P_e$  cut-off value for positive BBB permeation. Panel B) Evaluation of cytotoxic effect of compounds on SH-SY5Y cells by MTT assay. Cells were incubated for 24 h in presence of 5 or 10  $\mu\text{M}$  of compounds 56, 57 and 59. Results represent the % of cell viability of treated cells referred to untreated ones. Panel C) Neuroprotection assay on SH-SY5Y cells. Cells were incubated with compounds 56, 57 and 59 at a 5  $\mu\text{M}$  concentration. After 1 h, ethacrynic acid (45  $\mu\text{M}$ ) was added and results represent the cell viability of treated cells referred to untreated ones after 24 h. Significant values are indicated with \* (p value < 0.1). (For interpretation of the references to color in this figure legend, the reader is referred to the web version of this article.)

inhibitors. In this work, due to the low potency of the developed compounds in terms of inhibitory activity towards the target kinase, selectivity has not been explored and will be investigated in a future work where, hopefully, optimized structures will be obtained. Encouragingly, our previous reported triazolo-triazine compound, even if bears an adenine like scaffold, demonstrated to be quite selective among kinases. [22].

### 3. Materials and methods

#### 3.1. Chemistry

##### 3.1.1. General chemistry

Reagents were obtained from commercial suppliers and used without further purification. Reactions were monitored by TLC, on precoated silica gel plates (Macherey-Nagel, 60FUV254) or aluminum oxide plates (Macherey-Nagel, 60FUV254). Final compounds and intermediates were purified by flash chromatography using as stationary phases silica gel (Macherey-Nagel, silica 60, 240–400 mesh) or aluminum oxide (Macherey-Nagel, aluminum oxide 90 neutral, 50–200  $\mu\text{m}$ ). When used, light petroleum ether refers to the fractions boiling at 40–60  $^{\circ}\text{C}$ . Melting

points were determined with a Stuart melting point apparatus SMP10, and they were not corrected. The  $^1\text{H}$  NMR and  $^{13}\text{C}$  NMR were recorded on Varian Gemini 200 MHz, Jeol GX 270 MHz or Varian 400 MHz spectrometers using  $\text{CDCl}_3$  or  $\text{DMSO}-d_6$  as deuterated solvents; chemical shifts ( $\delta$  scale) are reported in parts per million (ppm) and referenced to residual solvent peak, with splitting patterns abbreviated to: s (singlet), d (doublet), dd (doublet of doublets), dt (doublet of triplets), t (triplet), m (multiplet) and bs (broad signal). Coupling constants (J) are given in Hz. MS-ESI analysis were performed using ESI Bruker 4000 Esquire spectrometer or microTOF-Q – Bruker, also used for accurate mass recording. HPLC analyses were performed using a SHIMADZU CBM-20-A, with a UV-vis detector set up at 254 nm, using a C18 column as stationary phase and methanol/ $\text{H}_2\text{O}$  as mobile one. All experiments were performed eluting the compound by gradient from methanol/ $\text{H}_2\text{O}$  45:55 to 85:15, with a flow of 1 mL/min in 20 min.

##### 3.1.2. Synthesis of 2,4,6-triphenoxy-1,3,5-triazine (2)

See reference [27].

##### 3.1.3. Synthesis of 2-hydrazineyl-4,6-diphenoxy-1,3,5-triazine (3)

See reference [27].

### 3.1.4. Synthesis of *N'*-(4,6-diphenoxy-1,3,5-triazin-2-yl)formohydrazide (4)

See reference [27].

### 3.1.5. General procedure for the synthesis of substituted *N'*-(4,6-diphenoxy-1,3,5-triazin-2-yl)hydrazides (5,8–11)

13.2 g of 2,4,6-triphenoxy-1,3,5-triazine (**2**, 37.0 mmol) and 7.82 g of required hydrazine (55.0 mmol) were dissolved in anhydrous THF (100 mL) and 8.22 mL of DBU (55.0 mmol) were added dropwise at 0 °C. The reaction was stirred at room temperature for 12 h. Once completed, the solvent was removed under reduced pressure and the crude residue was solved in DCM (100 mL) and washed with water (100 mL x 3). The organic layer was concentrated under reduced pressure, dried over sodium sulfate and purified with flash chromatography.

*N'*-(4,6-diphenoxy-1,3,5-triazin-2-yl)acetohydrazide (**5**): flash chromatography eluent: DCM 100 % to DCM-MeOH 1 %. Yield 28 %; white solid; mp 214–215 °C; <sup>1</sup>H NMR (270 MHz, DMSO-*d*<sub>6</sub>) δ 9.81 (s, 2H), 7.52–7.35 (m, 4H), 7.35–7.14 (m, 6H), 1.76 (s, 3H). ES-MS (methanol) *m/z*: 338.5 [M+H]<sup>+</sup>, 360.5 [M+Na]<sup>+</sup>.

*N'*-(4,6-diphenoxy-1,3,5-triazin-2-yl)thiophene-2-carbohydrazide (**8**): flash chromatography eluent: DCM-EtOAc 5 % to DCM-EtOAc 20 %. Yield 76 %; white solid; mp 207–210 °C; <sup>1</sup>H NMR (270 MHz, DMSO-*d*<sub>6</sub>) δ 10.53 (bs, 1H), 10.07 (bs, 1H), 7.88 (d, *J*=4.9 Hz, 1H), 7.75 (d, *J*=3.5 Hz, 1H), 7.44 (t, *J*=7.7 Hz, 2H), 7.37–6.99 (m, 9H). ES-MS (methanol) *m/z*: 406.0 [M+H]<sup>+</sup>, 427.9 [M+Na]<sup>+</sup>, 443.9 [M+K]<sup>+</sup>.

*N'*-(4,6-diphenoxy-1,3,5-triazin-2-yl)benzohydrazide (**9**): see reference [22].

3-chloro-*N'*-(4,6-diphenoxy-1,3,5-triazin-2-yl)benzohydrazide (**10**): flash chromatography eluent: DCM to DCM-EtOAc 10 %. Yield 67 %; white solid; mp 222–223 °C; <sup>1</sup>H NMR (200 MHz, DMSO-*d*<sub>6</sub>) δ 10.56 (s, 1H), 10.12 (s, 1H), 7.90–6.98 (m, 14H).

*N'*-(4,6-diphenoxy-1,3,5-triazin-2-yl)-3-nitrobenzohydrazide (**11**): flash chromatography eluent: DCM to DCM-MeOH 5 %. Yield 15 %; white solid; mp 201–202 °C; <sup>1</sup>H NMR (200 MHz, DMSO-*d*<sub>6</sub>) δ 10.81 (s, 1H), 10.21 (s, 1H), 8.57–8.36 (m, 2H), 8.15 (d, *J*=7.6 Hz, 1H), 7.80 (t, *J*=7.9 Hz, 1H), 7.56–6.97 (m, 10H).

### 3.1.6. General procedure for the synthesis of *N'*-(4,6-diphenoxy-1,3,5-triazin-2-yl)cycloalkylcarbohydrazides (6,7)

1.0 mmol of desired cycloalkylcarboxylic acid was solved in DCM (1.5 mL/mmol of carboxylic acid) and 1.2 mmol of oxalylchloride were added to the mixture. The reaction was stirred at room temperature for 30 min, then refluxed for 3–4 h. The solvent was removed under reduced pressure and the crude residue was used in the following step without further purification.

1.0 mmol of 2-hydrazineyl-4,6-diphenoxy-1,3,5-triazine (**3**) and 1.0 mmol of TEA were solved in DCM (4 mL/mmol of **3**) and the reaction was stirred at 0 °C. A solution of 1.5 mmol of cycloalkylcarbonyl chloride prepared in DCM (2 mL/mmol) was added dropwise for 2 h at 0 °C. The reaction was stirred at room temperature for 12 h. Once completed, the solvent was removed under reduced pressure and crude residue was filtered using EtOEt and light petroleum.

*N'*-(4,6-diphenoxy-1,3,5-triazin-2-yl)cyclobutanecarbohydrazide (**6**): flash chromatography eluent: DCM-MeOH 2 % to DCM-MeOH 10 %. Yield 74 %; white solid; mp 209–212 °C. <sup>1</sup>H NMR (400 MHz, DMSO-*d*<sub>6</sub>) δ 9.75 (s, 1H), 9.62 (s, 1H), 7.52–7.33 (m, 4H), 7.33–7.03 (m, 6H), 2.91 (d, *J*=8.1 Hz, 1H), 2.12–1.61 (m, 6H). ES-MS (methanol) *m/z*: 378.2 [M+H]<sup>+</sup>, 400.1 [M+Na]<sup>+</sup>, 416.1 [M+K]<sup>+</sup>.

*N'*-(4,6-diphenoxy-1,3,5-triazin-2-yl)cyclopentane-carbohydrazide (**7**): flash chromatography eluent: DCM-MeOH 3 % to DCM-MeOH 10 %. Yield 66 %; white solid; mp 208–210 °C. <sup>1</sup>H NMR (270 MHz, DMSO-*d*<sub>6</sub>) δ 9.73 (d, *J*=11.1 Hz, 2H), 7.52–7.33 (m, 4H), 7.33–7.06 (m, 6H), 2.49–2.33 (m, 1H), 1.79–1.29 (m, 8H). ES-MS (methanol) *m/z*: 391.8 [M+H]<sup>+</sup>, 413.9 [M+Na]<sup>+</sup>, 429.8 [M+K]<sup>+</sup>.

### 3.1.7. General procedure for the synthesis of 5,7-diphenoxy-[1,2,4]triazolo[1,5-*a*][1,3,5]triazines (12–19)

A mixture of 0.045 mol phosphorous pentoxide and 0.045 mol of hexamethyldisiloxane was suspended in 150 mL of anhydrous xylene and heated to 90 °C over 1.5 h, then was stirred at 90 °C for 1 h. Then 0.015 mol of well dried 2-hydrazineyl-4,6-diphenoxy-1,3,5-triazines (**4–11**) were added to the clear solution and refluxed for 2–4 h. Once completed, the solvent was removed under reduced pressure and the residue was solved in 300.0 mL of DCM and washed with water (3 x 100.0 mL). The organic layer was concentrated, dried over sodium sulfate and purified.

5,7-diphenoxy-[1,2,4]triazolo[1,5-*a*][1,3,5]triazine (**12**): see reference [27].

2-methyl-5,7-diphenoxy-[1,2,4]triazolo[1,5-*a*][1,3,5]triazine (**13**): flash chromatography eluent: light petroleum 50 %-EtOAc 50 %. Yield 26 %; white solid; mp 180–181 °C. <sup>1</sup>H NMR (200 MHz, DMSO-*d*<sub>6</sub>) δ 7.62–7.36 (m, 7H), 7.35–7.13 (m, 3H), 2.46 (s, 3H). <sup>13</sup>C NMR (50 MHz, DMSO-*d*<sub>6</sub>) δ 166.00, 163.81, 159.80, 154.30, 151.68, 150.34, 129.89 (2C), 129.55 (2C), 127.08, 125.82, 121.30 (4C), 14.70. ES-MS (acetonitrile) *m/z*: 320.5 [M+H]<sup>+</sup>, 342.4 [M+Na]<sup>+</sup>, 358.4 [M+K]<sup>+</sup>.

2-cyclobutyl-5,7-diphenoxy-[1,2,4]triazolo[1,5-*a*][1,3,5]triazine (**14**): flash chromatography eluent: DCM 100 % to DCM-EtOAc 10 %. Yield 32 %; white solid; mp 154–155 °C. <sup>1</sup>H NMR (400 MHz, DMSO-*d*<sub>6</sub>) δ 7.56 (t, *J*=7.7 Hz, 2H), 7.51–7.35 (m, 5H), 7.30 (t, *J*=7.4 Hz, 1H), 7.22 (d, *J*=8.3 Hz, 2H), 3.71 (p, *J*=8.5 Hz, 1H), 2.42–2.25 (m, 4H), 2.17–2.01 (m, 1H), 1.99–1.84 (m, 1H). <sup>13</sup>C NMR (68 MHz, DMSO-*d*<sub>6</sub>) δ 172.12, 164.24, 160.19, 154.91, 152.05, 150.70, 130.17 (2C), 129.82 (2C), 127.36, 126.10, 121.60 (4C), 33.48, 26.95 (2C), 18.26. ES-MS (acetonitrile) *m/z*: 360.0 [M+H]<sup>+</sup>, 382.1 [M+Na]<sup>+</sup>, 398.1 [M+K]<sup>+</sup>. HRMS (ESI-TOF) *m/z*: C<sub>20</sub>H<sub>17</sub>N<sub>5</sub>O<sub>2</sub> theoretical 360.1455 [M+H]<sup>+</sup>, experimental 360.1453 [M+H]<sup>+</sup> (Δ = 0.0002). Purity HPLC 97.0 %.

2-cyclopentyl-5,7-diphenoxy-[1,2,4]triazolo[1,5-*a*][1,3,5]triazine (**15**): flash chromatography eluent: DCM-light petroleum 5 % to DCM-EtOAc 5 %. Yield 29 %; white solid; mp 155–160 °C. <sup>1</sup>H NMR (270 MHz, CDCl<sub>3</sub>) δ 7.50 (t, *J*=7.7 Hz, 2H), 7.37 (t, *J*=8.1 Hz, 5H), 7.31–7.20 (m, 1H), 7.16 (d, *J*=7.8 Hz, 2H), 3.36 (p, *J*=8.1 Hz, 1H), 2.27–1.54 (m, 8H). <sup>13</sup>C NMR (68 MHz, DMSO-*d*<sub>6</sub>) δ 173.28, 164.21, 160.08, 154.81, 152.05, 150.69, 130.14 (2C), 129.80 (2C), 127.34, 126.07, 121.60 (4C), 38.77, 31.61 (2C), 25.26 (2C). ES-MS (acetonitrile) *m/z*: 374.0 [M+H]<sup>+</sup>, 396.0 [M+Na]<sup>+</sup>, 412.0 [M+K]<sup>+</sup>. HRMS (ESI-TOF) *m/z*: C<sub>21</sub>H<sub>19</sub>N<sub>5</sub>O<sub>2</sub> theoretical 374.1612 [M+H]<sup>+</sup>, experimental 374.1610 [M+H]<sup>+</sup> (Δ = 0.0002). Purity HPLC 94.5 %.

5,7-diphenoxy-2-(thiophen-2-yl)-[1,2,4]triazolo[1,5-*a*][1,3,5]triazine (**16**): flash chromatography eluent: DCM 100 % to DCM-EtOAc 2 %. Yield 63 %; white solid; mp 258–261 °C. <sup>1</sup>H NMR (270 MHz, DMSO-*d*<sub>6</sub>) δ 7.89 (d, *J*=2.5 Hz, 1H), 7.85 (d, *J*=5.0 Hz, 1H), 7.65–7.39 (m, 7H), 7.38–7.21 (m, 4H). <sup>13</sup>C NMR (68 MHz, DMSO-*d*<sub>6</sub>) δ 164.58, 161.65, 160.40, 155.03, 151.99, 150.70, 132.37, 130.23 (2C), 129.87 (2C), 129.54, 129.38, 128.78, 127.45, 126.20, 121.59 (4C). ES-MS (methanol) *m/z*: 388.1 [M+H]<sup>+</sup>, 410.1 [M+Na]<sup>+</sup>. HRMS (ESI-TOF) *m/z*: C<sub>20</sub>H<sub>13</sub>N<sub>5</sub>O<sub>2</sub>S theoretical 410.0682 [M+Na]<sup>+</sup>, experimental 410.0683 [M+Na]<sup>+</sup> (Δ = 0.0001). Purity HPLC 89.7 %.

5,7-diphenoxy-2-phenyl-[1,2,4]triazolo[1,5-*a*][1,3,5]triazine (**17**): see reference [22].

2-(3-chlorophenyl)-5,7-diphenoxy-[1,2,4]triazolo[1,5-*a*][1,3,5]triazine (**18**): flash chromatography eluent: DCM-light petroleum 20 %. Yield 65 %; white solid; mp 247–249 °C. <sup>1</sup>H NMR (200 MHz, DMSO-*d*<sub>6</sub>) δ 8.16 (s, 2H), 7.74–7.15 (m, 12H). <sup>13</sup>C NMR (50 MHz, DMSO-*d*<sub>6</sub>) δ 164.21 (s), 163.71 (s), 160.20 (s), 154.88 (s), 151.64 (s), 150.36 (s), 133.75 (s), 131.85–130.56 (m, 2C), 129.81 (d, *J*=17.9 Hz, 2C), 127.23 (s), 126.86–125.00 (m), 121.33 (s, 4C). ES-MS (methanol) *m/z*: C<sub>22</sub>H<sub>14</sub>ClN<sub>5</sub>O<sub>2</sub> theoretical 416.1 [M+H]<sup>+</sup>, 438.1 [M+Na]<sup>+</sup>, 454.0 [M+K]<sup>+</sup>, experimental 416.1 [M+H]<sup>+</sup>, 438.1 [M+Na]<sup>+</sup>, 454.0 [M+K]<sup>+</sup>.

2-(3-nitrophenyl)-5,7-diphenoxy-[1,2,4]triazolo[1,5-*a*][1,3,5]triazine (**19**): flash chromatography eluent: DCM 90 %-light petroleum 10 % to DCM-MeOH 0.5 %. Yield 9 %; white solid; mp 239–242 °C. <sup>1</sup>H



NMR (200 MHz, DMSO- $d_6$ )  $\delta$  8.90 (s, 1H), 8.62 (d,  $J=7.5$  Hz, 1H), 8.43 (dd,  $J=7.8, 1.5$  Hz, 1H), 7.90 (t,  $J=8.0$  Hz, 1H), 7.68–7.18 (m, 10H).  $^{13}\text{C}$  NMR (50 MHz, DMSO- $d_6$ )  $\delta$  164.41, 163.22, 160.44, 155.01, 151.70, 150.43, 148.31, 132.95, 131.04, 130.05, 129.70, 127.31, 126.07, 125.64, 121.36. ES-MS (methanol)  $m/z$ :  $\text{C}_{22}\text{H}_{14}\text{N}_6\text{O}_4$  theoretical 427.1  $[\text{M}+\text{H}]^+$ , 449.1  $[\text{M}+\text{Na}]^+$ , 465.1  $[\text{M}+\text{K}]^+$ , experimental 427.2  $[\text{M}+\text{H}]^+$ , 449.1  $[\text{M}+\text{Na}]^+$ , 465.1  $[\text{M}+\text{K}]^+$ .

### 3.1.8. General procedure for the synthesis of 5-phenoxy-[1,2,4]triazolo[1,5-*a*][1,3,5]triazin-7-amine (20–27)

1.0 g of 5,7-diphenoxy-[1,2,4]triazolo[1,5-*a*][1,3,5]triazine (12–19) was dissolved in 100 mL of methanol; then 5 mL of ammonia 7 N methanol were added to the mixture and the reaction was stirred for 2–4 h. The solvent was removed under reduced pressure and crude residue was purified with flash chromatography affording products 20–27.

5-phenoxy-[1,2,4]triazolo[1,5-*a*][1,3,5]triazin-7-amine (20): see reference [27].

2-methyl-5-phenoxy-[1,2,4]triazolo[1,5-*a*][1,3,5]triazin-7-amine (21): flash chromatography eluent: DCM-EtOAc 10 %. Yield 84 %; white solid; mp 240–244 °C.  $^1\text{H}$  NMR (270 MHz, DMSO- $d_6$ )  $\delta$  8.97 (bs, 1H), 8.680 (bs, 1H), 7.51–7.37 (m, 2H), 7.36–7.17 (m, 3H), 2.37 (s, 3H). ES-MS (acetonitrile)  $m/z$ :  $\text{C}_{11}\text{H}_{10}\text{N}_6\text{O}$  theoretical 243.1  $[\text{M}+\text{H}]^+$ , 265.1  $[\text{M}+\text{Na}]^+$ , 281.1  $[\text{M}+\text{K}]^+$ , experimental 243.4  $[\text{M}+\text{H}]^+$ , 265.4  $[\text{M}+\text{Na}]^+$ , 281.4  $[\text{M}+\text{K}]^+$ .

2-cyclobutyl-5-phenoxy-[1,2,4]triazolo[1,5-*a*][1,3,5]triazin-7-amine (22): flash chromatography eluent: DCM-EtOAc 5 % to DCM-EtOAc 30 %. Yield 96 %; white solid; mp 198–200 °C.  $^1\text{H}$  NMR (400 MHz, DMSO- $d_6$ )  $\delta$  8.98 (s, 1H), 8.66 (s, 1H), 7.45 (t,  $J=7.9$  Hz, 2H), 7.33–7.14 (m, 3H), 3.61 (p,  $J=8.5$  Hz, 1H), 2.42–2.20 (m, 4H), 2.12–1.81 (m, 2H). ES-MS (acetonitrile)  $m/z$ : 283.1  $[\text{M}+\text{H}]^+$ , 305.1  $[\text{M}+\text{Na}]^+$ , 321.1  $[\text{M}+\text{K}]^+$ . HRMS (ESI-TOF)  $m/z$ :  $\text{C}_{14}\text{H}_{15}\text{N}_6\text{S}$  theoretical 283.1302  $[\text{M}+\text{H}]^+$ , experimental 283.1300  $[\text{M}+\text{H}]^+$  ( $\Delta = 0.0002$ ). Purity HPLC 96.4 %.

2-cyclopentyl-5-phenoxy-[1,2,4]triazolo[1,5-*a*][1,3,5]triazin-7-amine (23): flash chromatography eluent: DCM-MeOH 2 % to DCM-MeOH 4 %. Yield 75 %; white solid; mp 189–190 °C.  $^1\text{H}$  NMR (270 MHz, DMSO- $d_6$ )  $\delta$  8.78 (bs, 2H), 7.44 (t,  $J=7.7$  Hz, 2H), 7.39–7.11 (m, 3H), 3.17 (p,  $J=7.8$  Hz, 1H), 2.09–1.90 (m, 2H), 1.91–1.46 (m, 6H); ES-MS (methanol)  $m/z$ : 297.1  $[\text{M}+\text{H}]^+$ , 319.0  $[\text{M}+\text{Na}]^+$ , 335.0  $[\text{M}+\text{K}]^+$ . HRMS (ESI-TOF)  $m/z$ :  $\text{C}_{15}\text{H}_{16}\text{N}_6\text{S}$  theoretical 297.1458  $[\text{M}+\text{H}]^+$ , experimental 297.1457  $[\text{M}+\text{H}]^+$  ( $\Delta = 0.0001$ ). Purity HPLC 99.4 %.

5-phenoxy-2-(thiophen-2-yl)-[1,2,4]triazolo[1,5-*a*][1,3,5]triazin-7-amine (24): flash chromatography eluent: DCM-MeOH 1 % to DCM-MeOH 10 %, Yield 80 %; white solid; mp 120–121 °C.  $^1\text{H}$  NMR (270 MHz, DMSO- $d_6$ )  $\delta$  9.10 (s, 1H), 8.78 (s, 1H), 7.76 (d,  $J=4.2$  Hz, 2H), 7.46 (t,  $J=7.7$  Hz, 2H), 7.38–7.10 (m, 4H).  $^{13}\text{C}$  NMR (68 MHz, DMSO- $d_6$ )  $\delta$  165.21, 160.29, 159.20, 152.64, 152.07, 133.13, 129.72 (2C), 129.60, 128.51, 128.46, 125.61, 121.98 (2C). ES-MS (methanol)  $m/z$ :  $\text{C}_{14}\text{H}_{10}\text{N}_6\text{OS}$  theoretical 311.1  $[\text{M}+\text{H}]^+$ , 333.1  $[\text{M}+\text{Na}]^+$ , 349.0  $[\text{M}+\text{K}]^+$ , experimental 311.1  $[\text{M}+\text{H}]^+$ , 333.0  $[\text{M}+\text{Na}]^+$ , 349.0  $[\text{M}+\text{K}]^+$ . Purity HPLC 99.5 %.

5-phenoxy-2-phenyl-[1,2,4]triazolo[1,5-*a*][1,3,5]triazin-7-amine (25): see reference [22].

2-(3-chlorophenyl)-5-phenoxy-[1,2,4]triazolo[1,5-*a*][1,3,5]triazin-7-amine (26): flash chromatography eluent: DCM 100 % to DCM-MeOH 1 %. Yield 93 %; white solid; mp 283–286 °C.  $^1\text{H}$  NMR (200 MHz, DMSO- $d_6$ )  $\delta$  9.00 (s, 2H), 8.08 (dd,  $J=9.9, 4.6$  Hz, 2H), 7.74–7.17 (m, 7H). ES-MS (methanol)  $m/z$ :  $\text{C}_{16}\text{H}_{11}\text{ClN}_6\text{O}$  theoretical 339.1  $[\text{M}+\text{H}]^+$ , experimental 339.3  $[\text{M}+\text{H}]^+$ .

2-(3-nitrophenyl)-5-phenoxy-[1,2,4]triazolo[1,5-*a*][1,3,5]triazin-7-amine (27): flash chromatography eluent: DCM 100 % to DCM-MeOH 5 %. Yield 96 %; white solid; mp 300 °C.  $^1\text{H}$  NMR (200 MHz, DMSO- $d_6$ )  $\delta$  9.22 (s, 1H), 8.93 (m, 2H), 8.62–8.28 (m, 2H), 7.86 (t,  $J=8.0$  Hz, 1H), 7.38 (m, 5H). ES-MS (acetonitrile)  $m/z$ :  $\text{C}_{16}\text{H}_{11}\text{N}_7\text{O}_3$  theoretical 350.1  $[\text{M}+\text{H}]^+$ , 372.1  $[\text{M}+\text{Na}]^+$ , 388.1  $[\text{M}+\text{K}]^+$ , experimental 350.1

$[\text{M}+\text{H}]^+$ , 364.2  $[\text{M}+\text{Na}]^+$ , 388.0  $[\text{M}+\text{K}]^+$ .

### 3.1.9. General procedure for the synthesis of 5-aminosubstituted-[1,2,4]triazolo[1,5-*a*][1,3,5]triazin-7-amine (28–73)

Method A: 1.0 mmol of 5-phenoxy-[1,2,4]triazolo[1,5-*a*][1,3,5]triazin-7-amine (20) was suspended in 6 mL of EtOH in a sealed tube. 3.0 mmol of desired amine was then added to the mixture and the reaction was heated to 90–95 °C for 12–72 h. Once completed, the solvent was removed under reduced pressure and the crude residue was purified with flash chromatography.

Method B: 1.0 mmol of 5-phenoxy-[1,2,4]triazolo[1,5-*a*][1,3,5]triazin-7-amine (20) was suspended in 6 mL of BuOH. 3.0 mmol of desired amine was then added to the mixture and the reaction was heated in microwave reactor to 170 °C for 1 h. Once completed, the solvent was removed under reduced pressure and the crude residue was purified with flash chromatography.

$\text{N}^5$ -(2-methylbenzyl)-[1,2,4]triazolo[1,5-*a*][1,3,5]triazine-5,7-diamine (28): method A. Flash chromatography eluent: DCM-MeOH 2 % to DCM-MeOH 3 %. Yield 48 %; white solid; mp 219–221 °C.  $^1\text{H}$  NMR (400 MHz, DMSO- $d_6$ )  $\delta$  8.41–7.99 (m, 3H), 7.87–7.79 (m, 1H), 7.26–7.08 (m, 4H), 4.51–4.43 (m, 2H), 2.34–2.26 (m, 3H).  $^{13}\text{C}$  NMR (101 MHz, DMSO- $d_6$ )  $\delta$  161.25, 158.77, 154.08, 150.27, 137.39, 135.24, 129.78, 126.69, 126.50, 125.64, 41.80, 18.68. ES-MS (methanol)  $m/z$ : 256.1  $[\text{M}+\text{H}]^+$ , 278.0  $[\text{M}+\text{Na}]^+$ , 294.0  $[\text{M}+\text{K}]^+$ . HRMS (ESI-TOF)  $m/z$ :  $\text{C}_{12}\text{H}_{13}\text{N}_7$  theoretical 278.1125  $[\text{M}+\text{Na}]^+$ , experimental 278.1123  $[\text{M}+\text{Na}]^+$  ( $\Delta = 0.0002$ ). HPLC Purity 97.1 %.

$\text{N}^5$ -(3-methylbenzyl)-[1,2,4]triazolo[1,5-*a*][1,3,5]triazine-5,7-diamine (29): method A. Flash chromatography eluent: DCM-MeOH 2.5 %. Yield 25 %; white solid; mp 217–219 °C.  $^1\text{H}$  NMR (270 MHz, DMSO- $d_6$ )  $\delta$  8.23–8.00 (m, 3H), 7.90–7.82 (m, 1H), 7.22–7.00 (m, 4H), 4.52–4.42 (m, 2H), 2.31–2.23 (m, 3H).  $^{13}\text{C}$  NMR (101 MHz, DMSO- $d_6$ )  $\delta$  179.52, 164.77, 162.46, 161.21 (CH), 139.85, 130.81, 128.10 (CH), 127.54 (CH), 127.20 (CH), 124.08 (CH), 45.71 (CH<sub>2</sub>), 21.05 (CH<sub>3</sub>). ES-MS (methanol)  $m/z$ : 256.1  $[\text{M}+\text{H}]^+$ , 278.0  $[\text{M}+\text{Na}]^+$ , 294.0  $[\text{M}+\text{K}]^+$ . HRMS (ESI-TOF)  $m/z$ :  $\text{C}_{12}\text{H}_{13}\text{N}_7$  theoretical 278.1125  $[\text{M}+\text{Na}]^+$ , experimental 278.1124  $[\text{M}+\text{Na}]^+$  ( $\Delta = 0.0001$ ). HPLC Purity 94.5 %.

$\text{N}^5$ -(4-methylbenzyl)-[1,2,4]triazolo[1,5-*a*][1,3,5]triazine-5,7-diamine (30): method A. Flash chromatography eluent: DCM-MeOH 3 % to DCM-MeOH 4 %. Yield 44 %; white solid; mp 277–279 °C.  $^1\text{H}$  NMR (270 MHz, DMSO- $d_6$ )  $\delta$  8.32–7.93 (m, 2H), 7.90–7.79 (m, 1H), 7.22–7.14 (m, 2H), 7.14–7.06 (m, 2H), 4.50–4.38 (m, 2H), 2.30–2.23 (s, 3H).  $^{13}\text{C}$  NMR (101 MHz, DMSO- $d_6$ )  $\delta$  161.22, 158.77, 154.08, 150.26, 136.86, 135.56, 128.72, 127.02, 43.47, 20.66. ES-MS (methanol)  $m/z$ : 255.9  $[\text{M}+\text{H}]^+$ , 277.6  $[\text{M}+\text{Na}]^+$ . HRMS (ESI-TOF)  $m/z$ :  $\text{C}_{12}\text{H}_{13}\text{N}_7$  theoretical 278.1125  $[\text{M}+\text{Na}]^+$ , experimental 278.1124  $[\text{M}+\text{Na}]^+$  ( $\Delta = 0.0001$ ). HPLC Purity 99.6 %.

In this reaction was obtained and purified also the derivative  $\text{N}^5, \text{N}^7$ -bis(4-methylbenzyl)-[1,2,4]triazolo[1,5-*a*][1,3,5]triazine-5,7-diamine (68): yield 12 %. White solid; mp 242–245 °C.  $^1\text{H}$  NMR (270 MHz, DMSO- $d_6$ )  $\delta$  9.22–8.98 (m, 1H), 8.14–8.06 (m, 1H), 8.07–7.98 (m, 1H), 7.33–6.97 (m, 8H), 4.63–4.48 (m, 2H), 4.48–4.37 (m, 2H), 2.34–2.19 (s, 6H). ES-MS (methanol)  $m/z$ : 360.0  $[\text{M}+\text{H}]^+$ , 382.0  $[\text{M}+\text{Na}]^+$ . HRMS (ESI-TOF)  $m/z$ :  $\text{C}_{20}\text{H}_{21}\text{N}_7$  theoretical 382.1751  $[\text{M}+\text{Na}]^+$ , experimental 382.1750  $[\text{M}+\text{Na}]^+$  ( $\Delta = 0.0001$ ). HPLC Purity 98.5 %.

$\text{N}^5$ -(2-methoxybenzyl)-[1,2,4]triazolo[1,5-*a*][1,3,5]triazine-5,7-diamine (31): method A. Flash chromatography eluent: DCM-MeOH 2 %. Yield 32 %; white solid; mp 220–221 °C.  $^1\text{H}$  NMR (400 MHz, DMSO- $d_6$ )  $\delta$  8.43–7.96 (m, 3H), 7.71–7.66 (m, 1H), 7.25–7.12 (m, 2H), 6.99–6.83 (m, 2H), 4.53–4.41 (m, 2H), 3.83 (s, 3H).  $^{13}\text{C}$  NMR (101 MHz, DMSO- $d_6$ )  $\delta$  161.81, 159.20, 156.93, 154.51, 150.70, 128.10, 127.55, 127.24, 120.48, 110.71, 55.70. ES-MS (methanol)  $m/z$ : 272.0  $[\text{M}+\text{H}]^+$ , 294.0  $[\text{M}+\text{Na}]^+$ . HRMS (ESI-TOF)  $m/z$ :  $\text{C}_{12}\text{H}_{13}\text{N}_7\text{O}$  theoretical 294.1074  $[\text{M}+\text{Na}]^+$ , experimental 294.1073  $[\text{M}+\text{Na}]^+$  ( $\Delta = 0.0001$ ).

$\text{N}^5$ -(3-methoxybenzyl)-[1,2,4]triazolo[1,5-*a*][1,3,5]triazine-5,7-diamine (32): method A. Flash chromatography eluent: DCM-MeOH 2.5 %. Yield 28 %; white solid; mp 208–210 °C.  $^1\text{H}$  NMR (400 MHz, DMSO-

$d_6$ )  $\delta$  8.32–7.99 (m, 3H), 7.93–7.87 (m, 1H), 7.24–7.20 (m, 1H), 6.92–6.85 (m, 2H), 6.81–6.78 (m, 1H), 4.52–4.43 (m, 2H), 3.76–3.68 (s, 3H). ES-MS (methanol)  $m/z$ : 272.1 [M+H]<sup>+</sup>, 294.0 [M+Na]<sup>+</sup>. HRMS (ESI-TOF)  $m/z$ : C<sub>12</sub>H<sub>13</sub>N<sub>7</sub>O theoretical 294.1074 [M+Na]<sup>+</sup>, experimental 294.1075 [M+Na]<sup>+</sup> ( $\Delta$  = 0.0001). HPLC Purity 100 %.

N<sup>5</sup>-(4-methoxybenzyl)-[1,2,4]triazolo[1,5-*a*][1,3,5]triazine-5,7-diamine (**33**): method A. Flash chromatography eluent: DCM-MeOH 2.5 %. Yield 55 %; white solid; mp 266–268 °C. <sup>1</sup>H NMR (270 MHz, DMSO-*d*<sub>6</sub>)  $\delta$  8.50–8.04 (m, 3H), 7.88–7.81 (m, 1H), 6.90–6.83 (m, 2H), 4.47–4.38 (m, 2H), 3.73–3.69 (s, 3H). <sup>13</sup>C NMR (101 MHz, DMSO-*d*<sub>6</sub>)  $\delta$  161.16, 158.78, 158.09, 154.08, 150.25, 131.81, 128.37, 113.59, 55.02, 43.17. ES-MS (methanol)  $m/z$ : 272.1 [M+H]<sup>+</sup>, 294.0 [M+Na]<sup>+</sup>. HRMS (ESI-TOF)  $m/z$ : C<sub>12</sub>H<sub>13</sub>N<sub>7</sub>O theoretical 294.1074 [M+Na]<sup>+</sup>, experimental 294.1072 [M+Na]<sup>+</sup> ( $\Delta$  = 0.0002). HPLC purity 98.9 %.

In this reaction was obtained and purified also the derivative N<sup>5</sup>,N<sup>7</sup>-bis(4-methoxybenzyl)-[1,2,4]triazolo[1,5-*a*][1,3,5]triazine-5,7-diamine (**69**): yield 16 %. White solid; mp 195–198 °C. <sup>1</sup>H NMR (270 MHz, DMSO-*d*<sub>6</sub>)  $\delta$  9.21–8.97 (m, 1H), 8.21–7.98 (m, 2H), 7.39–7.13 (m, 4H), 6.94–6.67 (m, 4H), 4.58–4.37 (m, 4H), 3.71 (s, 6H). ES-MS (methanol)  $m/z$ : 392.1 [M+H]<sup>+</sup>, 414.1 [M+Na]<sup>+</sup>. HRMS (ESI-TOF)  $m/z$ : C<sub>20</sub>H<sub>21</sub>N<sub>7</sub>O<sub>2</sub> theoretical 414.1649 [M+Na]<sup>+</sup>, experimental 414.1649 [M+Na]<sup>+</sup> ( $\Delta$  = 0.0000). HPLC purity 96.4 %.

N<sup>5</sup>-(3,4-dimethoxybenzyl)-[1,2,4]triazolo[1,5-*a*][1,3,5]triazine-5,7-diamine (**34**): method A. Flash chromatography eluent: DCM-MeOH 2.5 %. Yield 25 %; white solid; mp 230–232 °C. <sup>1</sup>H NMR (400 MHz, DMSO-*d*<sub>6</sub>)  $\delta$  8.06 (m, 2H), 7.88–7.72 (m, 1H), 6.96 (s, 1H), 6.90–6.78 (m, 2H), 4.48–4.35 (m, 2H), 3.74–3.67 (m, 6H). <sup>13</sup>C NMR (101 MHz, DMSO-*d*<sub>6</sub>)  $\delta$  161.14, 158.77, 154.09, 150.25, 148.58, 147.64, 132.24, 119.15, 111.68, 111.30, 55.55, 55.41, 43.55. ES-MS (methanol)  $m/z$ : 302.0 [M+H]<sup>+</sup>, 324.0 [M+Na]<sup>+</sup>. HRMS (ESI-TOF)  $m/z$ : C<sub>13</sub>H<sub>15</sub>N<sub>7</sub>O<sub>2</sub> theoretical 324.1179 [M+Na]<sup>+</sup>, experimental 324.1178 [M+Na]<sup>+</sup> ( $\Delta$  = 0.0001). HPLC Purity 99.4 %.

N<sup>5</sup>-(2-chlorobenzyl)-[1,2,4]triazolo[1,5-*a*][1,3,5]triazine-5,7-diamine (**35**): method A. Flash chromatography eluent: DCM-MeOH 2.5 %. Yield 15 %; white solid; mp 203–205 °C. <sup>1</sup>H NMR (400 MHz, DMSO-*d*<sub>6</sub>)  $\delta$  8.53–8.01 (m, 3H), 7.92–7.88 (m, 2H), 7.46–7.42 (m, 1H), 7.36–7.24 (m, 5H), 4.59–4.51 (m, 2H). ES-MS (methanol)  $m/z$ : 276.0 [M+H]<sup>+</sup>, 298.0 [M+Na]<sup>+</sup>. HRMS (ESI-TOF)  $m/z$ : C<sub>11</sub>H<sub>10</sub>ClN<sub>7</sub> theoretical 298.0578 [M+Na]<sup>+</sup>, experimental 298.0579 [M+Na]<sup>+</sup> ( $\Delta$  = 0.0001). HPLC Purity 99.7 %.

N<sup>5</sup>-(3-chlorobenzyl)-[1,2,4]triazolo[1,5-*a*][1,3,5]triazine-5,7-diamine (**36**): method A. Flash chromatography eluent: EtOAc 70 %-light petroleum 30 %. Yield 33 %; white solid; mp 216–218 °C. <sup>1</sup>H NMR (400 MHz, DMSO-*d*<sub>6</sub>)  $\delta$  8.53–8.02 (m, 2H), 8.01–7.89 (m, 1H), 7.43–7.19 (m, 3H), 4.58–4.42 (m, 2H). ES-MS (methanol)  $m/z$ : 276.0 [M+H]<sup>+</sup>, 298.0 [M+Na]<sup>+</sup>. <sup>13</sup>C NMR (101 MHz, DMSO-*d*<sub>6</sub>)  $\delta$  167.62, 161.64, 154.53, 150.78, 143.10, 133.33, 130.55, 127.21, 126.16, 109.99, 43.68. HPLC Purity 99.5 %.

In this reaction was obtained and purified also the derivative N<sup>5</sup>,N<sup>7</sup>-bis(3-chlorobenzyl)-[1,2,4]triazolo[1,5-*a*][1,3,5]triazine-5,7-diamine (**70**): yield 10 %. White solid; mp 207–210 °C. <sup>1</sup>H NMR (270 MHz, DMSO-*d*<sub>6</sub>)  $\delta$  9.67–8.70 (m, 1H), 8.12 (s, 1H), 7.64–6.86 (m, 8H), 4.81–4.36 (m, 4H). HRMS (ESI-TOF)  $m/z$ : C<sub>18</sub>H<sub>15</sub>Cl<sub>2</sub>N<sub>7</sub> theoretical 400.0839 [M+H]<sup>+</sup>, experimental 400.0838 [M+H]<sup>+</sup> ( $\Delta$  = 0.0001). HPLC Purity 100 %.

N<sup>5</sup>-(4-chlorobenzyl)-[1,2,4]triazolo[1,5-*a*][1,3,5]triazine-5,7-diamine (**37**): method A. Flash chromatography eluent: DCM-MeOH 4 %. Yield 40 %; white solid; mp 243–246 °C. <sup>1</sup>H NMR (400 MHz, DMSO-*d*<sub>6</sub>)  $\delta$  8.34–8.00 (m, 3H), 7.97–7.91 (m, 1H), 7.41–7.31 (m, 4H), 4.53–4.44 (m, 2H). <sup>13</sup>C NMR (101 MHz, DMSO-*d*<sub>6</sub>)  $\delta$  161.64, 159.14, 154.52, 150.76, 139.46, 131.53, 129.33 (2C), 128.57 (2C), 43.56. ES-MS (methanol)  $m/z$ : 275.9 [M+H]<sup>+</sup>, 297.8 [M+Na]<sup>+</sup>. HRMS (ESI-TOF)  $m/z$ : C<sub>11</sub>H<sub>10</sub>ClN<sub>7</sub> theoretical 298.0578 [M+Na]<sup>+</sup>, experimental 298.0578 [M+Na]<sup>+</sup> ( $\Delta$  = 0.0000).

N<sup>5</sup>-(2-fluorobenzyl)-[1,2,4]triazolo[1,5-*a*][1,3,5]triazine-5,7-diamine (**38**): method A. Flash chromatography eluent: light petroleum

70 %-EtOAc 30 %. Yield 21 %; white solid; mp 254–256 °C. <sup>1</sup>H NMR (270 MHz, DMSO-*d*<sub>6</sub>)  $\delta$  8.45–7.94 (m, 2H), 7.92–7.80 (m, 1H), 7.42–7.24 (m, 2H), 7.23–6.99 (m, 2H), 4.66–4.40 (m, 2H). <sup>13</sup>C NMR (101 MHz, DMSO-*d*<sub>6</sub>)  $\delta$  161.21 (d,  $J$ =9.7 Hz), 158.72 (d,  $J$ =6.4 Hz), 154.09, 150.34, 128.96 (d,  $J$ =4.4 Hz), 128.57 (d,  $J$ =7.9 Hz), 126.53, 126.38, 124.25, 114.94 (d,  $J$ =21.1 Hz), 37.63 (d,  $J$ =5.0 Hz). ES-MS (methanol)  $m/z$ : 260.0 [M+H]<sup>+</sup>, 282.0 [M+Na]<sup>+</sup>. HRMS (ESI-TOF)  $m/z$ : C<sub>11</sub>H<sub>10</sub>FN<sub>7</sub> theoretical 282.0874 [M+Na]<sup>+</sup>, experimental 282.0874 [M+Na]<sup>+</sup> ( $\Delta$  = 0.0000). HPLC Purity 98.1 %.

N<sup>5</sup>-(3-fluorobenzyl)-[1,2,4]triazolo[1,5-*a*][1,3,5]triazine-5,7-diamine (**39**): method A. Flash chromatography eluent: light petroleum 70 %-EtOAc 30 %. Yield 20 %; white solid; mp 251–253 °C. <sup>1</sup>H NMR (400 MHz, DMSO-*d*<sub>6</sub>)  $\delta$  8.33–8.02 (m, 3H), 7.96–7.92 (m, 1H), 7.38–7.33 (m, 2H), 7.16–7.02 (m, 2H), 4.54–4.47 (m, 2H). ES-MS (methanol)  $m/z$ : 260.0 [M+H]<sup>+</sup>, 282.0 [M+Na]<sup>+</sup>. HRMS (ESI-TOF)  $m/z$ : C<sub>11</sub>H<sub>10</sub>FN<sub>7</sub> theoretical 282.0874 [M+Na]<sup>+</sup>, experimental 282.0874 [M+Na]<sup>+</sup> ( $\Delta$  = 0.0000). HPLC Purity 94.5 %.

N<sup>5</sup>-(4-fluorobenzyl)-[1,2,4]triazolo[1,5-*a*][1,3,5]triazine-5,7-diamine (**40**): method A. Flash chromatography eluent: DCM-MeOH 2.5 % to DCM-MeOH 3 %. Yield 57 %; white solid; mp 218–221 °C. <sup>1</sup>H NMR (270 MHz, DMSO-*d*<sub>6</sub>)  $\delta$  8.56–7.95 (m, 2H), 7.97–7.82 (m, 1H), 7.43–7.25 (m, 2H), 7.26–7.00 (m, 2H), 4.59–4.35 (m, 2H). <sup>13</sup>C NMR (101 MHz, DMSO-*d*<sub>6</sub>)  $\delta$  162.29, 161.20, 159.88, 158.74, 154.09, 150.29, 136.10, 128.98 (d,  $J$ =7.9 Hz), 114.89 (d,  $J$ =21.1 Hz), 43.04. ES-MS (methanol)  $m/z$ : 260.0 [M+H]<sup>+</sup>, 281.7 [M+Na]<sup>+</sup>. HRMS (ESI-TOF)  $m/z$ : C<sub>11</sub>H<sub>10</sub>FN<sub>7</sub> theoretical 282.0874 [M+Na]<sup>+</sup>, experimental 282.0875 [M+Na]<sup>+</sup> ( $\Delta$  = 0.0001). HPLC Purity 99.7 %.

In this reaction was obtained and purified also the derivative N<sup>5</sup>,N<sup>7</sup>-bis(4-fluorobenzyl)-[1,2,4]triazolo[1,5-*a*][1,3,5]triazine-5,7-diamine (**71**): yield 23 %. White solid; mp 243–244 °C. <sup>1</sup>H NMR (270 MHz, DMSO-*d*<sub>6</sub>)  $\delta$  9.26–9.04 (m, 1H), 8.13–8.03 (m, 2H), 7.49–6.97 (m, 8H), 4.64–4.50 (m, 2H), 4.51–4.43 (m, 2H). <sup>13</sup>C NMR (101 MHz, DMSO-*d*<sub>6</sub>)  $\delta$  162.86 (d,  $J$ =22.2 Hz), 161.47 (d,  $J$ =25.0 Hz), 159.05, 154.75 (d,  $J$ =35.6 Hz), 149.28, 136.49 (d,  $J$ =41.3 Hz), 135.02, 130.29–129.11 (m), 115.51 (d,  $J$ =16.3 Hz), 115.31 (d,  $J$ =16.2 Hz), 43.58, 42.98. ES-MS (methanol)  $m/z$ : 368.1 [M+H]<sup>+</sup>, 390.0 [M+Na]<sup>+</sup>. HRMS (ESI-TOF)  $m/z$ : C<sub>18</sub>H<sub>15</sub>F<sub>2</sub>N<sub>7</sub> theoretical 368.1430 [M+H]<sup>+</sup>, experimental 368.1432 [M+H]<sup>+</sup> ( $\Delta$  = 0.0002). HPLC Purity 95.9 %.

N<sup>5</sup>-(pyridin-4-ylmethyl)-[1,2,4]triazolo[1,5-*a*][1,3,5]triazine-5,7-diamine (**41**): method A. Flash chromatography eluent: DCM-MeOH 5 % to DCM-MeOH 7 %. Yield 52 %; white solid; mp 279–280 °C. <sup>1</sup>H NMR (400 MHz, DMSO-*d*<sub>6</sub>)  $\delta$  8.61–8.42 (m, 2H), 8.42–8.04 (m, 3H), 8.01–7.92 (m, 1H), 7.33–7.27 (m, 2H), 4.58–4.47 (m, 2H). <sup>13</sup>C NMR (101 MHz, DMSO-*d*<sub>6</sub>)  $\delta$  161.75, 159.08, 154.54, 150.82, 149.86, 149.48, 122.42, 43.35. ES-MS (methanol)  $m/z$ : 243.0 [M+H]<sup>+</sup>, 264.9 [M+Na]<sup>+</sup>. HRMS (ESI-TOF)  $m/z$ : C<sub>10</sub>H<sub>10</sub>N<sub>8</sub> theoretical 243.1101 [M+H]<sup>+</sup>, experimental 243.1101 [M+H]<sup>+</sup> ( $\Delta$  = 0.0000). HPLC Purity 99.8 %.

N<sup>5</sup>-phenethyl-[1,2,4]triazolo[1,5-*a*][1,3,5]triazine-5,7-diamine (**42**): method A. Flash chromatography eluent: DCM-MeOH 4 %. Yield 51 %; white solid; mp 174–176 °C. <sup>1</sup>H NMR (270 MHz, DMSO-*d*<sub>6</sub>)  $\delta$  8.16–7.98 (m, 3H), 7.48–7.40 (m, 1H), 7.32–7.18 (m, 5H), 3.60–3.40 (m, 2H), 2.91–2.78 (m, 2H). <sup>13</sup>C NMR (101 MHz, DMSO-*d*<sub>6</sub>)  $\delta$  161.45, 159.26, 154.49, 150.60, 140.06, 129.11 (2C), 128.73 (2C), 126.46, 42.57, 35.20. ES-MS (methanol)  $m/z$ : 256.0 [M+H]<sup>+</sup>, 278.0 [M+Na]<sup>+</sup>. HRMS (ESI-TOF)  $m/z$ : C<sub>12</sub>H<sub>13</sub>N<sub>7</sub> theoretical 278.1125 [M+Na]<sup>+</sup>, experimental 278.1125 [M+Na]<sup>+</sup> ( $\Delta$  = 0.0000). HPLC Purity 99.7 %.

In this reaction was obtained and purified also the derivative N<sup>5</sup>,N<sup>7</sup>-diphenethyl-[1,2,4]triazolo[1,5-*a*][1,3,5]triazine-5,7-diamine (**72**): yield 14 %. White solid; mp 209–213 °C. <sup>1</sup>H NMR (270 MHz, DMSO-*d*<sub>6</sub>)  $\delta$  8.86–8.46 (m, 2H), 8.12–8.03 (m, 1H), 7.67–7.55 (m, 1H), 7.56–6.40 (m, 10H), 3.85–3.38 (m, 4H), 3.11–2.63 (m, 4H). ES-MS (methanol)  $m/z$ : 359.9 [M+H]<sup>+</sup>, 381.9 [M+Na]<sup>+</sup>. HRMS (ESI-TOF)  $m/z$ : C<sub>20</sub>H<sub>21</sub>N<sub>7</sub> theoretical 382.1751 [M+Na]<sup>+</sup>, experimental 382.1750 [M+Na]<sup>+</sup> ( $\Delta$  = 0.0001). HPLC Purity 97.9 %.

N<sup>5</sup>-(cyclohexylmethyl)-[1,2,4]triazolo[1,5-*a*][1,3,5]triazine-5,7-diamine (**43**): method A. Flash chromatography eluent: DCM-MeOH 2

%. Yield 39 %; white solid; mp 215–217 °C.  $^1\text{H}$  NMR (400 MHz, DMSO- $d_6$ )  $\delta$  8.08–7.88 (m, 3H), 7.49–7.34 (m, 1H), 3.16–3.04 (m, 2H), 1.78–1.45 (m, 6H), 1.25–1.07 (m, 3H), 0.97–0.75 (m, 2H). ES-MS (methanol)  $m/z$ : 247.9 [M+H] $^+$ , 269.9 [M+Na] $^+$ .  $^{13}\text{C}$  NMR (101 MHz, DMSO- $d_6$ )  $\delta$  161.69, 159.27, 154.45, 150.47, 47.20 (CH $_2$ ), 37.42, 30.95 (2CH $_2$ ), 26.57 (CH $_2$ ), 25.86 (2CH $_2$ ). HRMS (ESI-TOF)  $m/z$ : C $_{11}$ H $_{17}$ N $_7$  theoretical 270.1438 [M+Na] $^+$ , experimental 270.1436 [M+Na] $^+$  ( $\Delta$  = 0.0002). HPLC Purity 99.8 %.

$\text{N}^5$ -benzyl-2-methyl-[1,2,4]triazolo[1,5-*a*][1,3,5]triazine-5,7-diamine (**44**): method A. Flash chromatography eluent: DCM-MeOH 0.1 % to DCM-MeOH 2 %. Yield 25 %; white solid; mp 165–167 °C.  $^1\text{H}$  NMR (270 MHz, DMSO- $d_6$ )  $\delta$  8.35–7.73 (m, 3H), 7.36–7.17 (m, 5H), 4.68–4.30 (m, 2H), 2.29 (s, 3H).  $^{13}\text{C}$  NMR (101 MHz, DMSO- $d_6$ )  $\delta$  162.99, 161.14, 159.11, 149.89, 140.02, 128.17, 127.02, 126.56, 44.10, 43.72, 14.56. ES-MS (acetonitrile)  $m/z$ : 256.5 [M+H] $^+$ , 278.4 [M+Na] $^+$ . HRMS (ESI-TOF)  $m/z$ : C $_{12}$ H $_{13}$ N $_7$  theoretical 278.1125 [M+Na] $^+$ , experimental 278.1124 [M+Na] $^+$  ( $\Delta$  = 0.0001). HPLC purity 97.4 %.

$\text{N}^5$ -cyclohexyl-2-methyl-[1,2,4]triazolo[1,5-*a*][1,3,5]triazine-5,7-diamine (**45**): method A. Flash chromatography eluent: DCM-MeOH 0.5 % to DCM-MeOH 2 %. Yield 32 %; white solid; mp 123–125 °C.  $^1\text{H}$  NMR (270 MHz, DMSO- $d_6$ )  $\delta$  8.32–7.79 (m, 2H), 7.36–7.04 (m, 1H), 3.71 (m, 1H), 2.26 (s, 3H), 1.91–1.46 (m, 5H), 1.38–0.96 (m, 5H).  $^{13}\text{C}$  NMR (101 MHz, DMSO- $d_6$ )  $\delta$  162.90, 160.16, 159.21, 150.39, 149.73, 49.39, 49.30–49.10 (m), 32.68, 32.28, 25.30, 24.87, 14.57. ES-MS (acetonitrile)  $m/z$ : 248.5 [M+H] $^+$ , 270.5 [M+Na] $^+$ , 286.4 [M+K] $^+$ . HRMS (ESI-TOF)  $m/z$ : C $_{11}$ H $_{17}$ N $_7$  theoretical 248.1618 [M+H] $^+$ , experimental 248.1619 [M+H] $^+$  ( $\Delta$  = 0.0001). HPLC purity 95.4 %.

$\text{N}^5$ -benzyl-2-cyclobutyl-[1,2,4]triazolo[1,5-*a*][1,3,5]triazine-5,7-diamine (**46**): method A. Flash chromatography eluent: DCM-MeOH 2 %. Yield 17 %; white solid; mp 166–170 °C.  $^1\text{H}$  NMR (400 MHz, DMSO- $d_6$ )  $\delta$  8.40–7.71 (m, 3H), 7.40–7.27 (m, 4H), 7.27–7.18 (m, 1H), 4.60–4.35 (m, 2H), 3.63–3.41 (m, 1H), 2.41–2.16 (m, 4H), 2.15–1.95 (m, 1H), 2.00–1.80 (m, 2H). ES-MS (methanol)  $m/z$ : 296.2 [M+H] $^+$ , 318.1 [M+Na] $^+$ . HRMS (ESI-TOF)  $m/z$ : C $_{15}$ H $_{17}$ N $_7$  theoretical 296.1618 [M+H] $^+$ , experimental 296.1616 [M+H] $^+$  ( $\Delta$  = 0.0002). HPLC purity 98.9 %.

2-cyclobutyl- $\text{N}^5$ -(3-methylbenzyl)-[1,2,4]triazolo[1,5-*a*][1,3,5]triazine-5,7-diamine (**47**): method B. Flash chromatography eluent: DCM-MeOH 1 % to DCM-MeOH 5 %. Yield 57 %; white solid; mp 220–221 °C.  $^1\text{H}$  NMR (400 MHz, DMSO- $d_6$ )  $\delta$  8.44–7.65 (m, 3H), 7.21–7.14 (m, 1H), 7.13–7.06 (m, 2H), 7.05–6.98 (m, 1H), 4.54–4.36 (m, 2H), 3.66–3.40 (m, 1H), 2.38–2.17 (m, 7H), 2.09–1.94 (m, 1H), 1.94–1.83 (m, 1H).  $^{13}\text{C}$  NMR (101 MHz, DMSO- $d_6$ )  $\delta$  168.99, 161.05, 159.11, 150.04, 140.00, 137.18, 128.09 (CH), 127.51 (CH), 127.18 (CH), 124.08 (CH), 43.68 (CH $_2$ ), 33.56 (CH), 27.01 (2 x CH $_2$ ), 21.06 (CH $_3$ ), 18.24 (CH $_2$ ). HRMS (ESI-TOF)  $m/z$ : C $_{16}$ H $_{19}$ N $_7$  theoretical 310.1775 [M+H] $^+$ , experimental 310.1773 [M+H] $^+$  ( $\Delta$  = 0.0002). HPLC purity: 95.1 %.

2-cyclobutyl- $\text{N}^5$ -phenethyl-[1,2,4]triazolo[1,5-*a*][1,3,5]triazine-5,7-diamine (**48**): method A. Flash chromatography eluent: DCM-MeOH 1.5 %. Yield 25 %; white solid; mp 185–188 °C.  $^1\text{H}$  NMR (400 MHz, DMSO- $d_6$ )  $\delta$  8.45–7.68 (m, 2H), 7.56–7.11 (m, 6H), 3.64–3.40 (m, 3H), 2.88–2.78 (m, 2H), 2.42–2.15 (m, 4H), 2.15–1.77 (m, 2H).  $^{13}\text{C}$  NMR (101 MHz, DMSO- $d_6$ )  $\delta$  168.97, 160.86, 159.19, 149.95, 139.66, 128.66, 128.30, 126.02, 42.16, 34.82, 33.58, 27.01, 18.24. ES-MS (methanol)  $m/z$ : 310.2 [M+H] $^+$ , 332.1 [M+Na] $^+$ , 348.1 [M+K] $^+$ . HRMS (ESI-TOF)  $m/z$ : C $_{16}$ H $_{19}$ N $_7$  theoretical 310.1775 [M+H] $^+$ , experimental 310.1771 [M+H] $^+$  ( $\Delta$  = 0.0004). HPLC purity 98.4 %.

2-cyclobutyl- $\text{N}^5$ -(cyclohexylmethyl)-[1,2,4]triazolo[1,5-*a*][1,3,5]triazine-5,7-diamine (**49**): method A. Flash chromatography eluent: DCM-MeOH 2 % to DCM-MeOH 3 %. Yield 24 %; white solid; mp 201–204 °C.  $^1\text{H}$  NMR (400 MHz, DMSO- $d_6$ )  $\delta$  7.91 (bs, 2H), 7.42–7.30 (m, 1H), 3.51 (p,  $J$ =8.5 Hz, 1H), 3.17–3.01 (m, 2H), 2.39–2.18 (m, 4H), 2.12–1.81 (m, 2H), 1.77–1.43 (m, 6H), 1.26–1.05 (m, 3H), 0.98–0.80 (m, 2H). ES-MS (methanol)  $m/z$ : 302.2 [M+H] $^+$ , 324.2 [M+Na] $^+$ , 340.1 [M+K] $^+$ . HRMS (ESI-TOF)  $m/z$ : C $_{15}$ H $_{23}$ N $_7$  theoretical 302.2088

[M+H] $^+$ , experimental 302.2084 [M+H] $^+$  ( $\Delta$  = 0.0004). HPLC purity 98.1 %.

$\text{N}^5$ -(*sec*-butyl)-2-cyclobutyl-[1,2,4]triazolo[1,5-*a*][1,3,5]triazine-5,7-diamine (**50**): method A. Flash chromatography eluent: light petroleum 60 %-EtOAc 40 % to light petroleum 40 %-EtOAc 60 %. Yield 19 %; white solid; mp 110–112 °C.  $^1\text{H}$  NMR (400 MHz, DMSO- $d_6$ )  $\delta$  7.87 (bs, 1H), 7.25–7.02 (m, 1H), 3.95–3.79 (m, 1H), 3.51 (p,  $J$ =8.6 Hz, 1H), 2.41–2.18 (m, 4H), 2.08–1.83 (m, 2H), 1.60–1.31 (m, 2H), 1.09 (d,  $J$ =6.5 Hz, 3H), 0.95–0.64 (m, 3H). ES-MS (methanol)  $m/z$ : 262.1 [M+H] $^+$ , 284.0 [M+Na] $^+$ . HRMS (ESI-TOF)  $m/z$ : C $_{12}$ H $_{19}$ N $_7$  theoretical 262.1775 [M+H] $^+$ , experimental 262.1775 [M+H] $^+$  ( $\Delta$  = 0.0000). HPLC purity 99.1 %.

$\text{N}^5$ -benzyl-2-cyclopentyl-[1,2,4]triazolo[1,5-*a*][1,3,5]triazine-5,7-diamine (**51**): method A. Flash chromatography eluent: light petroleum 60 %-EtOAc 40 % to light petroleum 50 %-EtOAc 50 %. Yield 30 %; white solid; mp 189–191 °C.  $^1\text{H}$  NMR (270 MHz, DMSO- $d_6$ )  $\delta$  8.40–7.62 (m, 3H), 7.47–7.02 (m, 5H), 4.47 (bs, 2H), 3.20–2.95 (m, 1H), 2.10–1.41 (m, 8H).  $^{13}\text{C}$  NMR (101 MHz, DMSO- $d_6$ )  $\delta$  170.34, 155.86, 153.72, 142.67, 140.52, 128.61 (2C), 127.40 (2C), 109.99, 44.14, 40.97, 32.11 (3C), 25.81 (2C). ES-MS (methanol)  $m/z$ : 310.1 [M+H] $^+$ , 332.1 [M+Na] $^+$ , 348.1 [M+K] $^+$ . HRMS (ESI-TOF)  $m/z$ : C $_{16}$ H $_{19}$ N $_7$  theoretical 310.1775 [M+H] $^+$ , experimental 310.1775 [M+H] $^+$  ( $\Delta$  = 0.0000). HPLC purity 97.8 %.

2-cyclopentyl- $\text{N}^5$ -(3-methylbenzyl)-[1,2,4]triazolo[1,5-*a*][1,3,5]triazine-5,7-diamine (**52**): method B. Flash chromatography eluent: DCM-MeOH 1 % to DCM-MeOH 2 %. Yield 56 %; white solid; mp 223–225 °C.  $^1\text{H}$  NMR (400 MHz, DMSO- $d_6$ )  $\delta$  8.54–7.58 (m, 3H), 7.18 (t,  $J$ =7.5 Hz, 1H), 7.13–7.05 (m, 2H), 7.02 (d,  $J$ =7.5 Hz, 1H), 4.54–4.36 (m, 2H), 3.08 (p,  $J$ =8.0 Hz, 1H), 2.27 (s, 3H), 2.02–1.87 (m, 2H), 1.87–1.52 (m, 6H).  $^{13}\text{C}$  NMR (101 MHz, DMSO- $d_6$ )  $\delta$  170.10, 161.03, 159.04, 149.96, 140.01, 137.18, 128.09, (CH) 127.48 (CH), 127.17 (CH), 124.05 (CH), 43.65 (CH $_2$ ), 38.68 (CH), 31.67 (CH $_2$ ), 25.37 (CH $_2$ ), 21.06 (CH $_3$ ). HRMS (ESI-TOF)  $m/z$ : C $_{17}$ H $_{21}$ N $_7$  theoretical 324.1931 [M+H] $^+$ , experimental 324.1930 [M+H] $^+$  ( $\Delta$  = 0.0001). HPLC purity: 95.5 %.

2-cyclopentyl- $\text{N}^5$ -phenethyl-[1,2,4]triazolo[1,5-*a*][1,3,5]triazine-5,7-diamine (**53**): method A. Flash chromatography eluent: DCM-MeOH 2 % to DCM-MeOH 10 %. Yield 27 %; white solid; mp 187–189 °C.  $^1\text{H}$  NMR (270 MHz, DMSO- $d_6$ )  $\delta$  7.91 (bs, 2H), 7.48–7.08 (m, 6H), 3.55–3.40 (m, 2H), 3.17–3.01 (m, 1H), 2.90–2.77 (m, 2H), 2.05–1.52 (m, 8H). ES-MS (methanol)  $m/z$ : 324.1 [M+H] $^+$ , 345.8 [M+Na] $^+$ . HRMS (ESI-TOF)  $m/z$ : C $_{17}$ H $_{23}$ N $_7$  theoretical 324.1931 [M+H] $^+$ , experimental 324.1933 [M+H] $^+$  ( $\Delta$  = 0.0002). HPLC purity 99.5 %.

$\text{N}^5$ -(cyclohexylmethyl)-2-cyclopentyl-[1,2,4]triazolo[1,5-*a*][1,3,5]triazine-5,7-diamine (**54**): method A. Flash chromatography eluent: DCM-MeOH 2 %. Yield 22 %; white solid; mp 211–215 °C.  $^1\text{H}$  NMR (270 MHz, DMSO- $d_6$ )  $\delta$  7.85 (bs, 2H), 7.38–7.21 (m, 1H), 3.19–2.93 (m, 3H), 2.10–1.37 (m, 14H), 1.31–1.04 (m, 3H), 0.99–0.76 (m, 2H). ES-MS (methanol)  $m/z$ : 316.2 [M+H] $^+$ , 338.1 [M+Na] $^+$ . HRMS (ESI-TOF)  $m/z$ : C $_{16}$ H $_{25}$ N $_7$  theoretical 316.2244 [M+H] $^+$ , experimental 316.2243 [M+H] $^+$  ( $\Delta$  = 0.0001). HPLC purity 95.3 %.

$\text{N}^5$ -(*sec*-butyl)-2-cyclopentyl-[1,2,4]triazolo[1,5-*a*][1,3,5]triazine-5,7-diamine (**55**): method A. Flash chromatography eluent: light petroleum 60 %-EtOAc 40 %. Yield 41 %; white solid; mp 209–211 °C.  $^1\text{H}$  NMR (400 MHz, DMSO- $d_6$ )  $\delta$  8.28–7.68 (m, 2H), 7.31–6.81 (m, 1H), 4.05–3.75 (m, 1H), 3.08 (p,  $J$ =8.1 Hz, 1H), 2.07–1.30 (m, 10H), 1.09 (d,  $J$ =6.5 Hz, 3H), 0.85 (t,  $J$ =7.4 Hz, 3H). ES-MS (methanol)  $m/z$ : 276.1 [M+H] $^+$ , 298.1 [M+Na] $^+$ , 314.1 [M+K] $^+$ . HRMS (ESI-TOF)  $m/z$ : C $_{13}$ H $_{21}$ N $_7$  theoretical 276.1931 [M+H] $^+$ , experimental 276.1930 [M+H] $^+$  ( $\Delta$  = 0.0001). HPLC purity 99.5 %.

$\text{N}^5$ -benzyl-2-(thiophen-2-yl)-[1,2,4]triazolo[1,5-*a*][1,3,5]triazine-5,7-diamine (**56**): method A. Flash chromatography eluent: DCM-MeOH 1 % to DCM-MeOH 10 %. Yield 23 %; white solid; mp 232 °C.  $^1\text{H}$  NMR (400 MHz, DMSO- $d_6$ )  $\delta$  8.54–7.87 (m, 3H), 7.70 (bs, 1H), 7.43–7.23 (m, 3H), 7.26–7.13 (m, 1H), 4.83–4.20 (m, 2H).  $^{13}\text{C}$  NMR (101 MHz, DMSO- $d_6$ )  $\delta$  161.25, 159.21, 158.97, 150.02, 139.93, 133.71, 128.61,

128.19, 128.07, 127.57, 127.08, 126.60, 43.78. ES-MS (methanol)  $m/z$ : 324.1 [M+H]<sup>+</sup>, 346.1 [M+Na]<sup>+</sup>, 362.0 [M+K]<sup>+</sup>. HRMS (ESI-TOF)  $m/z$ : C<sub>15</sub>H<sub>13</sub>N<sub>7</sub>S theoretical 324.1025 [M+H]<sup>+</sup>, experimental 324.1026 [M+H]<sup>+</sup> ( $\Delta = 0.0001$ ). Purity HPLC 98.7 %.

N<sup>5</sup>-(2-methylbenzyl)-2-(thiophen-2-yl)-[1,2,4]triazolo[1,5-a][1,3,5]triazine-5,7-diamine (**57**): method B. Flash chromatography eluent: DCM-MeOH 1 % to DCM-MeOH 2 %. Yield 67 %; white solid; mp 253–254 °C. <sup>1</sup>H NMR (400 MHz, DMSO-*d*<sub>6</sub>)  $\delta$  8.50 – 7.93 (m, 2H), 8.00 – 7.80 (m, 1H), 7.80 – 7.54 (m, 2H), 7.38 – 7.03 (m, 5H), 4.64 – 4.34 (m, 2H), 2.46 – 2.22 (m, 3H). <sup>13</sup>C NMR (101 MHz, DMSO-*d*<sub>6</sub>)  $\delta$  161.25 (s), 159.20 (s), 158.97 (s), 149.99 (s), 137.39 (s), 135.23 (s), 133.69 (s), 129.77 (s, CH), 128.59 (s, CH), 128.05 (s, CH), 127.55 (s, CH), 126.77 (s, CH, 2C), 126.49 (s, CH, 2C), 125.64 (s, CH), 54.91 (s, CH<sub>2</sub>), 18.71 (s, CH<sub>3</sub>). HRMS (ESI-TOF)  $m/z$ : C<sub>16</sub>H<sub>15</sub>N<sub>7</sub>S theoretical 338.1182 [M+H]<sup>+</sup>, experimental 338.1184 [M+H]<sup>+</sup> ( $\Delta = 0.0002$ ). HPLC purity: 95.4 %.

N<sup>5</sup>-(3-methylbenzyl)-2-(thiophen-2-yl)-[1,2,4]triazolo[1,5-a][1,3,5]triazine-5,7-diamine (**58**): method B. Flash chromatography eluent: DCM-MeOH 1 % to DCM-MeOH 2 %. Yield 34 %; white solid; mp 227–229 °C. <sup>1</sup>H NMR (400 MHz, DMSO-*d*<sub>6</sub>)  $\delta$  8.52 – 7.85 (m, 3H), 7.70 (d,  $J=4.5$  Hz, 2H), 7.24 – 7.16 (m, 2H), 7.17 – 7.07 (m, 2H), 7.08 – 6.99 (m, 1H), 4.56 – 4.39 (m, 2H), 2.28 (s, 3H). <sup>13</sup>C NMR (101 MHz, DMSO-*d*<sub>6</sub>)  $\delta$  161.22, 159.21, 158.97, 149.99, 139.85, 137.20, 133.70, 128.59 (CH), 128.10 (CH), 128.05 (CH), 127.59 (CH), 127.55 (CH), 127.23 (CH), 124.16 (CH), 43.75 (CH<sub>2</sub>), 21.06 (CH<sub>3</sub>). HRMS (ESI-TOF)  $m/z$ : C<sub>16</sub>H<sub>15</sub>N<sub>7</sub>S theoretical 338.1182 [M+H]<sup>+</sup>, experimental 338.1181 [M+H]<sup>+</sup> ( $\Delta = 0.0001$ ). HPLC purity: 95.1 %.

N<sup>5</sup>-(3-methoxybenzyl)-2-(thiophen-2-yl)-[1,2,4]triazolo[1,5-a][1,3,5]triazine-5,7-diamine (**59**): method B. Flash chromatography eluent: DCM-MeOH 1 %. Yield 44 %; white solid; mp 203–204 °C. <sup>1</sup>H NMR (400 MHz, DMSO-*d*<sub>6</sub>)  $\delta$  8.53 – 7.87 (m, 3H), 7.70 (d,  $J=4.4$  Hz, 2H), 7.29 – 7.14 (m, 2H), 6.97 – 6.83 (m, 2H), 6.79 (dd,  $J=7.4, 2.1$  Hz, 1H), 4.58 – 4.37 (m, 2H), 3.73 (s, 3H). <sup>1</sup>H NMR (400 MHz, DMSO-*d*<sub>6</sub> @ 80 °C)  $\delta$  7.89 (s, 2H), 7.78 – 7.55 (m, 3H), 7.36 – 7.08 (m, 2H), 7.01 – 6.87 (m, 2H), 6.78 (dd,  $J=8.2, 2.2$  Hz, 1H), 4.50 (d,  $J=6.3$  Hz, 2H), 3.73 (s, 3H). <sup>13</sup>C NMR (101 MHz, DMSO-*d*<sub>6</sub>)  $\delta$  161.24, 159.25, 159.19, 158.98, 150.02, 141.55, 133.70, 129.25 (CH), 128.60 (CH), 128.06 (CH), 127.57 (CH), 119.24 (CH), 112.80 (CH), 111.85 (CH), 54.96 (CH<sub>3</sub>), 43.76 (CH<sub>2</sub>). HRMS (ESI-TOF)  $m/z$ : C<sub>16</sub>H<sub>15</sub>N<sub>7</sub>OS theoretical 354.1133 [M+H]<sup>+</sup>, experimental 354.1132 [M+H]<sup>+</sup> ( $\Delta = 0.0001$ ). HPLC purity: 97.2 %.

N<sup>5</sup>-phenethyl-2-(thiophen-2-yl)-[1,2,4]triazolo[1,5-a][1,3,5]triazine-5,7-diamine (**60**): method A. Flash chromatography eluent: DCM-MeOH 1 % to DCM-MeOH 2 %. Yield 35 %; white solid; mp 217–218 °C. <sup>1</sup>H NMR (270 MHz, DMSO-*d*<sub>6</sub>)  $\delta$  8.62 – 7.81 (m, 2H), 7.80 – 7.67 (m, 2H), 7.62 – 7.38 (m, 1H), 7.39 – 7.01 (m, 6H), 3.64 – 3.41 (m, 2H), 2.86 (t,  $J=6.5$  Hz, 2H). ES-MS (methanol)  $m/z$ : 337.9 [M+H]<sup>+</sup>, 359.8 [M+Na]<sup>+</sup>, 375.8 [M+K]<sup>+</sup>. HRMS (ESI-TOF)  $m/z$ : C<sub>16</sub>H<sub>15</sub>N<sub>7</sub>S theoretical 338.1182 [M+H]<sup>+</sup>, experimental 338.1184 [M+H]<sup>+</sup> ( $\Delta = 0.0002$ ). HPLC purity 97.6 %.

In this reaction was obtained and purified also the derivative N<sup>5</sup>,N<sup>7</sup>-diphenethyl-2-(thiophen-2-yl)-[1,2,4]triazolo[1,5-a][1,3,5]triazine-5,7-diamine (**73**): yield 9 %; white solid; mp 193–195 °C. <sup>1</sup>H NMR (270 MHz, DMSO-*d*<sub>6</sub>)  $\delta$  8.72 (bt,  $J=6.3$  Hz, 1H), 8.51 (bt,  $J=5.3$  Hz, 1H), 7.87 – 7.56 (m, 3H), 7.44 – 7.03 (m, 10H), 3.84 – 3.44 (m, 4H), 3.09 – 2.80 (m, 4H). <sup>13</sup>C NMR (101 MHz, DMSO-*d*<sub>6</sub>)  $\delta$  160.85, 159.08, 148.78, 148.31, 139.56, 138.98, 133.70, 128.83 – 127.94 (m), 127.65, 127.59, 126.23, 126.06, 42.22, 41.60, 35.52, 34.79. ES-MS (methanol)  $m/z$ : 441.9 [M+H]<sup>+</sup>, 463.8 [M+Na]<sup>+</sup>. HRMS (ESI-TOF)  $m/z$ : C<sub>24</sub>H<sub>23</sub>N<sub>7</sub>S theoretical 442.1808 [M+H]<sup>+</sup>, experimental 442.1802 [M+H]<sup>+</sup> ( $\Delta = 0.0006$ ). HPLC Purity 94.3 %.

N<sup>5</sup>-(cyclohexylmethyl)-2-(thiophen-2-yl)-[1,2,4]triazolo[1,5-a][1,3,5]triazine-5,7-diamine (**61**): method A. Flash chromatography eluent: DCM-MeOH 1 %. Yield 54 %; white solid; mp 257–259 °C. <sup>1</sup>H NMR (270 MHz, DMSO-*d*<sub>6</sub>)  $\delta$  8.56 – 7.88 (m, 2H), 7.83 – 7.61 (m, 2H), 7.65 – 7.34 (m, 0H), 7.36 – 7.08 (m, 1H), 3.10 (bs, 2H), 1.98 – 1.36 (m, 6H), 1.35 – 1.04 (m, 3H), 1.06 – 0.65 (m, 2H). <sup>13</sup>C NMR (101 MHz,

DMSO-*d*<sub>6</sub>)  $\delta$  161.27, 159.28, 158.92, 149.79, 133.81, 128.53, 128.02, 127.48, 46.79, 37.01, 30.52, 26.13, 25.42. ES-MS (methanol)  $m/z$ : 329.8 [M+H]<sup>+</sup>, 351.8 [M+Na]<sup>+</sup>. HRMS (ESI-TOF)  $m/z$ : C<sub>15</sub>H<sub>19</sub>N<sub>7</sub>S theoretical 330.1495 [M+H]<sup>+</sup>, experimental 330.1498 [M+H]<sup>+</sup> ( $\Delta = 0.0003$ ). HPLC purity 98.4 %.

N<sup>5</sup>-(*sec*-butyl)-2-(thiophen-2-yl)-[1,2,4]triazolo[1,5-a][1,3,5]triazine-5,7-diamine (**62**): method A. Flash chromatography eluent: light petroleum 60 %-EtOAc 40 %. Yield 32 %; white solid; mp 180–185 °C. <sup>1</sup>H NMR (400 MHz, DMSO-*d*<sub>6</sub>)  $\delta$  8.63 – 7.80 (m, 2H), 7.70 (d,  $J=4.0$  Hz, 2H), 7.26 (d,  $J=8.3$  Hz, 1H), 7.24 – 7.11 (m, 1H), 4.05 – 3.77 (m, 1H), 1.64 – 1.36 (m, 2H), 1.11 (d,  $J=6.3$  Hz, 3H), 0.87 (t,  $J=7.3$  Hz, 3H). <sup>13</sup>C NMR (101 MHz, DMSO-*d*<sub>6</sub>)  $\delta$  160.68, 159.30, 158.92, 149.81, 133.83, 128.51, 128.04, 127.47, 47.59, 28.60, 19.93, 10.69. ES-MS (methanol)  $m/z$ : 289.8 [M+H]<sup>+</sup>, 311.8 [M+Na]<sup>+</sup>. HRMS (ESI-TOF)  $m/z$ : C<sub>12</sub>H<sub>15</sub>N<sub>7</sub>S theoretical 290.1182 [M+H]<sup>+</sup>, experimental 290.1180 [M+H]<sup>+</sup> ( $\Delta = 0.0002$ ). HPLC purity 100 %.

N<sup>5</sup>-cyclohexyl-2-phenyl-[1,2,4]triazolo[1,5-a][1,3,5]triazine-5,7-diamine (**63**): method A. Flash chromatography eluent: DCM-MeOH 0.5 % to 1 %. Yield 31 %; white solid; mp 280–282 °C. <sup>1</sup>H NMR (200 MHz, DMSO-*d*<sub>6</sub>)  $\delta$  8.31–7.84 (m, 4H), 7.61–7.41 (m, 3H), 7.32 (d,  $J=8.1$  Hz, 1H), 3.88–3.61 (m, 1H), 2.01–1.47 (m, 5H), 1.45–1.01 (m, 5H). ES-MS (methanol)  $m/z$ : 310.2 [M+H]<sup>+</sup>, 332.2 [M+Na]<sup>+</sup>. HRMS (ESI-TOF)  $m/z$ : C<sub>16</sub>H<sub>20</sub>N<sub>7</sub> theoretical 310.1775 [M+H]<sup>+</sup>, experimental 310.1773 [M+H]<sup>+</sup> ( $\Delta = 0.0002$ ). HPLC purity 90.2 %.

N<sup>5</sup>-benzyl-2-(3-chlorophenyl)-[1,2,4]triazolo[1,5-a][1,3,5]triazine-5,7-diamine (**64**): method A. Flash chromatography eluent: DCM 100 % to DCM-MeOH 1 %. Yield 31 %; white solid; mp 257–259 °C. <sup>1</sup>H NMR (270 MHz, DMSO-*d*<sub>6</sub>)  $\delta$  8.09 – 7.56 (m, 2H), 7.55 – 7.52 (m, 2H), 7.33 – 7.22 (m, 5H), 4.53 – 4.50 (m, 2H). <sup>13</sup>C NMR (101 MHz, DMSO-*d*<sub>6</sub>)  $\delta$  161.32, 161.28, 159.46, 150.15, 139.90, 133.47, 130.82, 129.87, 128.11, 127.07, 126.61, 126.12, 125.14, 43.81. ES-MS (methanol)  $m/z$ : 352.1 [M+H]<sup>+</sup>, 374.1 [M+Na]<sup>+</sup>. HRMS (ESI-TOF)  $m/z$ : C<sub>17</sub>H<sub>14</sub>ClN<sub>7</sub> theoretical 374.0891 [M+Na]<sup>+</sup>, experimental 374.0891 [M+Na]<sup>+</sup> ( $\Delta = 0.0000$ ). HPLC purity 99.8 %.

2-(3-chlorophenyl)-N<sup>5</sup>-cyclohexyl-[1,2,4]triazolo[1,5-a][1,3,5]triazine-5,7-diamine (**65**): method A. Flash chromatography eluent: DCM-MeOH 0.5 %. Yield 29 %; white solid; mp 287–289 °C. <sup>1</sup>H NMR (400 MHz, DMSO-*d*<sub>6</sub>)  $\delta$  8.53 – 7.99 (m, 4H), 7.66 – 7.49 (m, 2H), 7.47 – 7.33 (m, 1H), 3.82 – 3.67 (m, 1H), 1.94 – 1.51 (m, 5H), 1.41 – 1.00 (m, 6H). ES-MS (methanol)  $m/z$ : 344.0 [M+H]<sup>+</sup>. HRMS (ESI-TOF)  $m/z$ : C<sub>16</sub>H<sub>18</sub>ClN<sub>7</sub> theoretical 344.1385 [M+H]<sup>+</sup>, experimental 344.1386 [M+H]<sup>+</sup> ( $\Delta = 0.0001$ ). HPLC Purity 97.1 %.

N<sup>5</sup>-benzyl-2-(3-nitrophenyl)-[1,2,4]triazolo[1,5-a][1,3,5]triazine-5,7-diamine (**66**): method A. Flash chromatography eluent: DCM 100 % to DCM-MeOH 0.5 %. Yield 30 %; white solid; mp 264–266 °C. <sup>1</sup>H NMR (270 MHz, DMSO-*d*<sub>6</sub>)  $\delta$  8.88 (s, 1H), 8.49 – 7.83 (m, 3H), 7.34 – 7.24 (m, 5H), 4.66 – 4.40 (m, 2H). ES-MS (methanol)  $m/z$ : 363.1 [M+H]<sup>+</sup>. HRMS (ESI-TOF)  $m/z$ : C<sub>17</sub>H<sub>14</sub>N<sub>8</sub>O<sub>2</sub> theoretical 385.1132 [M+Na]<sup>+</sup>, experimental 385.1133 [M+Na]<sup>+</sup> ( $\Delta = 0.0001$ ). HPLC purity 95.4 %.

N<sup>5</sup>-cyclohexyl-2-(3-nitrophenyl)-[1,2,4]triazolo[1,5-a][1,3,5]triazine-5,7-diamine (**67**): method A. Flash chromatography eluent: DCM-MeOH 0.5 %. Yield 17 %; white solid; mp 282–284 °C. <sup>1</sup>H NMR (270 MHz, DMSO-*d*<sub>6</sub>)  $\delta$  8.94 – 8.79 (m, 1H), 8.54 – 8.39 (m, 1H), 8.39 – 8.26 (m, 1H), 8.25 – 7.98 (m, 1H), 7.92 – 7.73 (m, 1H), 7.55 – 7.32 (m, 1H), 3.89 – 3.59 (m, 1H), 2.00 – 1.48 (m, 5H), 1.42 – 0.97 (m, 5H). ES-MS (methanol)  $m/z$ : 355.0 [M+H]<sup>+</sup>, 377.0 [M+Na]<sup>+</sup>, 393.0 [M+K]<sup>+</sup>. HRMS (ESI-TOF)  $m/z$ : C<sub>16</sub>H<sub>18</sub>N<sub>8</sub>O<sub>2</sub> theoretical 355.1625 [M+H]<sup>+</sup>, experimental 355.1626 [M+H]<sup>+</sup> ( $\Delta = 0.0001$ ). HPLC purity 90.5 %.

## 3.2. Computational studies

### 3.2.1. Protein preparation

The CK1 $\delta$  ligand–protein complex for the computational evaluation was chosen based on the cross-docking experiment carried on in a recent study by Pavan & Menin et. al. [37], and the PDB code of interest is the 4TN6. Specifically, the structure was downloaded from the Protein Data



Bank [38] and imported into the main window of the Molecular Operating Environment (MOE) [39] suite. Then, the system was prepared with the Structure preparation tool, which was exploited to give each amino acid side chain the right conformational state based on the occupancy. Then, the Protonate 3D application was used to properly assign each amino acid its appropriate protonation state at pH 7.4. Finally, the added hydrogen atoms were energetically minimized under the AMBER10:EHT [40] force field implemented in MOE.

### 3.2.2. Ligand preparation and molecular docking

The 52 ligands of the database under evaluation were all properly prepared to exploit the tools of the QUACPAC [41] package included in the OpenEye suite. First, the dominant tautomeric state was assigned to each molecule with the tautomer's application, then the three-dimensional coordinates for the compounds were generated with Omega. The partial charges for each molecular candidate were calculated with the MolCharge tool, using MMFF94 as the method. Finally, the dominant protonation state at pH 7.4 was selected by exploiting the FixpKa application. The molecular docking calculations were executed with the program PLANTS, based on an Ant Colony Optimization (ACO) algorithm, developed and released by the University of Tübingen [42].

### 3.2.3. System preparation for molecular Dynamics simulations

Each of the 44 protein–ligand systems coming from the post-docking filtration was properly prepared for molecular dynamics simulation based on the Amber force field. First, each ligand pose was assigned the appropriate partial charges using the AM1-BCC method using tleap. Then, each protein–ligand complex was solvated within a water box of 15 Å padding, using the explicit TIP3P [43] solvation model, and then neutralized with the addition of Na<sup>+</sup>/Cl<sup>-</sup> ions until a concentration of 0.154 M was reached. Then, each system underwent a 1000 steps energy minimization procedure, which was followed by a two-step equilibration. The first equilibration was executed in the canonical ensemble (NVT) for 0.1 ns, keeping a harmonic positional restraint of 5 kcal mol<sup>-1</sup> Å<sup>-2</sup> on both the protein and the ligand atoms. Then, the second equilibration was carried on in the isothermal-isobaric ensemble (NPT) for 0.5 ns, this time maintaining the harmonic positional restraint of 5 kcal mol<sup>-1</sup> Å<sup>-2</sup> just on the ligand and the protein α-carbon atoms. Then, three 10 ns MD simulations for each protein–ligand complex were executed, without any energetic constrain on the atoms, using ACEMD3 as the MD program, which is based on Open MM. For the NVT ensemble, the temperature was kept at the constant value of 310 K using the Langevin thermostat, while in the NPT equilibration the pressure was maintained at 1.0 atm exploiting a Monte Carlo barostat. For each simulation, a 2 fs integration time step was used. The bonds involving hydrogen atoms were constrained using the M–SHAKE algorithm, and a cutoff of 9.0 Å was adopted for the computation of the Lennard-Jones interactions. For the calculation of the electrostatic interaction, the particle-mesh Ewald method (PME) was exploited.

### 3.2.4. Analysis of the molecular Dynamics simulations

Each of the three replicas produced for each ligand was analyzed using an in-house build python script in order to extrapolate the main geometric and energetic information for the protein–ligand interaction. The RMSD and the RMSF were calculated with the python Prody package [44]. The electrostatic, the van der Waals, and the total interaction energies were computed using NAMDEnergy plugin (version 1.4) [45], and the MM/GBSA calculations were performed exploiting the appropriate tool available in the AMBER package.

## 3.3. Biology

### 3.3.1. CK1δ activity assay

The assays were performed following procedures reported in literature using truncated CK1δ (Merck Millipore, recombinant human, GST-tagged, aa 1–294) with the KinaseGlo® kit (Promega) [20]. Compounds

were screened in white 96-well plates at 30 °C in a final volume of 40 μL, using the following buffer: 50 mM HEPES (pH 7.5), 1 mM EDTA, 1 mM EGTA, 15 mM MgCl<sub>2</sub>. The candidate inhibitors were dissolved in DMSO (10 mM starting solution) and then diluted in the assay buffer to the desired concentration (the final DMSO concentration in the reaction mixture did not exceed 1 %). The compound PF-670462 (IC<sub>50</sub> = 14 nM) [14] was used as a positive control, while a DMSO/buffer solution was used as a negative control. In a typical assay, 10 μL of inhibitor solution and 10 μL of CK1δ (6.5 nM, final concentration) were added to each well, then 20 μL of assay buffer containing the substrates, casein (Sigma-Aldrich, casein solution from bovine milk, 5 % in water) and ATP, at a final concentration of 0.05 % and 2 μM respectively, were added. The reaction was incubated for 1 h at 30 °C, afterwards it was stopped by adding 40 μL of KinaseGlo reagent. The luminescence signal (relative light unit, RLU) was recorded after 10 min at 25 °C using Tecan Infinite M100. First, residual enzyme activity percentage was determined at 40 μM for each inhibitor with respect to DMSO/buffer only, and at 10 μM for compounds showing enzyme residual activity lower than 50 % at 40 μM. The percentage of inhibition was calculated on the basis of maximal activities measured in the absence of inhibitor and related to the difference between the total and consumed ATP, following this equation:

$$\text{Inhibition (\%)} = \frac{(\text{RLU}_x - \text{RLU}_{\text{CTRL-}}) / (\text{RLU}_{\text{CTRL+}} - \text{RLU}_{\text{CTRL-}})}{\bullet 100}$$

where RLU<sub>x</sub> is the luminescence signal measured in the well of the test compound, RLU<sub>CTRL-</sub> the luminescence measured in absence of inhibitor, RLU<sub>CTRL+</sub> the luminescence recorded for the reference compound PF-670462, at a concentration that ensures total enzyme inhibition (40 μM). Subsequently, for the most active compounds the IC<sub>50</sub> values were determined using ten different inhibitor concentrations ranging from 100 to 0.026 μM. Data were analyzed using Excel and GraphPad Prism software (version 8.0).

### 3.3.2. ATP-competition assay

The kinetic ATP-competition experiments have been performed by reporting the reciprocal of the used ATP in x-axis and the reciprocal of consumed ATP divided for total volume of the reaction (40 μL) in y-axis. Enzymatic activity has been determined using the same luciferase-based assay (Kinase Glo®) used to determine potency of compounds. The elaboration has been carried out by assaying compound 57 at the concentrations of 2.0 μM and 4.0 μM, corresponding to about 1x and 2x the IC<sub>50</sub> value of compound on CK1δ (IC<sub>50</sub> = 2.08 μM), using increasing ATP concentrations (1 μM, 5 μM, 10 μM, 50 μM).

### 3.3.3. PAMPA – BBB assay

The prediction of CNS permeation of our compounds was evaluated using a parallel artificial membrane permeability assay (PAMPA) adapted for BBB penetration evaluation [34]. Nine commercial drugs (Atenolol, Caffeine, Desipramine, Enoxacin, Hydrocortisone, Ofloxacin, Piroxicam, Testosterone, and Verapamil) were dissolved in EtOH (1 mL) and used as test compounds. The analysis set was validated through the linear correlation of literature and experimental data referring to these reference compounds (Fig. S5 and Table S3). The stock solutions were redissolved in PBS pH=7.4 buffer/EtOH 7:3. For tested inhibitors, 1–2 mg of every compound were dissolved in PBS/EtOH 7:3 and all the solutions were then filtered with PDVF membrane filters (0.45 μm pore size). 180 μL of PBS/EtOH 7:3 were added to each well of the acceptor 96-well microplate (MultiScreen 96-well Culture Tray clear, Merck Millipore) while the donor 96-well plate (Multiscreen® IP Sterile Plate PDVF membrane, pore size 0.45 μm) was coated with 4 μL of porcine brain lipid (Avanti Polar Lipids) in dodecane (20 mg/mL). After 10 min, 180 μL of compound solutions were added and the donor plate was then put on the acceptor plate to form a “sandwich”. During the incubation time (150 min at 25 °C) compounds diffused from the donor plate through the brain lipid membrane into the acceptor plate.

After incubation, the donor plate was removed and the UV absorbance in the acceptor plate was determined with UV plate reader Tecan Infinite M1000. Absorbance values from the donor plate (before incubation) and the acceptor plate were correlated with experiment parameters (well volume, membrane area, time of incubation) to calculate Pe values ( $10^{-6}$  cm/s). Every sample was analyzed at different absorption wavelengths, in 3 wells and two independent experiments. Results are given as the mean  $\pm$  standard deviation (SD).

### 3.3.4. Cell viability assay (MTT assay)

Human neuroblastoma SH-SY5Y cell line was propagated in Dulbecco's Modified Eagle Medium (DMEM) containing L-glutamine (2 mM), 1 % non-essential amino acids, 1 % penicillin/streptomycin and 10 % fetal bovine serum (FBS) under humidified 5 % CO<sub>2</sub>. Once semi-confluence was achieved, cells were counted using TC10™ Automated Cell Counter Bio-Rad Laboratories (CSIC-Madrid) and 80,000 cells/well were plated in a 96-well plate. After 24 h of incubation, compounds have been inserted at the concentrations of 5 and 10  $\mu$ M (DMSO stock solution was diluted with DMEM to obtain the desired final concentration). After another 24 h of incubation, DMEM was removed and MTT reagent (3-(4,5-dimethylthiazol-2-yl)-2,5-diphenyltetrazolium bromide) was added at the concentration of 20 mg/mL. After 2 h, absorbance was recorded, and cell survival estimated as percentage of value of untreated control (mean of six wells). Three independent experiments have been carried out.

### 3.3.5. Neuroprotection assay

Human neuroblastoma SH-SY5Y cell line was propagated in Dulbecco's Modified Eagle Medium (DMEM) containing L-glutamine (2 mM), 1 % non-essential amino acids, 1 % penicillin/streptomycin and 10 % fetal bovine serum (FBS) under humidified 5 % CO<sub>2</sub>. When semi-confluence was achieved, cells were counted using TC10™ Automated Cell Counter Bio-Rad Laboratories (CSIC-Madrid) and 60,000 cells/well were plated in a 96-well plate. After 24 h of incubation, compounds were added at the concentrations of 5 and 10  $\mu$ M (DMSO stock solutions were diluted with DMEM to obtain the desired final concentration) and after 1 h ethacrynic acid (45  $\mu$ M final concentration starting from a 100 mM stock solution diluted in DMEM) was added. As negative control, a solution of 1 % DMSO in DMEM was used while ethacrynic acid without compound was the positive control. After 24 h of incubation, DMEM was removed and MTT reagent (3-(4,5-dimethylthiazol-2-yl)-2,5-diphenyltetrazolium bromide) was added at the concentration of 20 mg/mL. After 2 h, absorbance was recorded and cell survival was estimated as the mean of relative absorbance of six wells/compound. Three independent experiments were performed, and statistical analysis of data was obtained using GraphPad Prism 8.0 one-way ANOVA for each plate and T-TEST to compare the three experiments.

## 4. Conclusions

In this work, the [1,2,4]triazolo[1,5-a][1,3,5]triazine scaffold has been investigated in order to obtain ATP-competitive CK1 $\delta$  inhibitors as potential neuroprotective agents. Attempts to make a structural optimization led to derivatives differently substituted at the 2 position with alkyl and aryl moieties, and at the 5 position with cycloalkyl and benzyl amines.

Only ten of the 47 developed compounds inhibit CK1 $\delta$  in the micromolar range, in particular, most potent compounds **51**, **56**, **57** and **59** proved to possess an IC<sub>50</sub> of 2.91, 2.55, 2.08 and 2.74  $\mu$ M towards CK1 $\delta$ , respectively. Three of them bear a thiophene ring at the 2 position, indicating that this substitution is undoubtedly favorable to gain interactions with the target. Computational studies identify one important feature for these series that could discriminate between active and inactive compounds: a chain composed of at least 2 atoms (e.g., nitrogen and carbon atoms) at the 5 position of the [1,2,4]triazolo[1,5-a][1,3,5]triazine triazolo might help the molecule to be correctly

oriented in the binding pocket, placing the nitrogen atoms in the correct position to form the characteristic bidentate hydrogen bond with Leu85. Indeed, most of the here reported compounds possess this feature, even resulting inactive. Unfortunately, nor docking nor MD studies allow a clear distinction between active and inactive compounds, suggesting that further studies are needed (e.g. the ongoing Supervised Molecular Dynamics studies).

Most active compounds **56**, **57** and **59** were preliminary assayed in a neuronal cell model of human neuroblastoma cells, where resulted to be safe when tested at a concentration of 10  $\mu$ M and compounds **57** and **59** were also neuroprotective on the same cell line when treated with the toxic agent, ethacrynic acid. These results, taken together with compounds' good permeability in the BBB-PAMPA assay and their objective low potency against the target, suggest that further optimization on the series could be very promising to the obtainment of neuroprotective agents to potentially treat neurodegenerative diseases.

## Funding

This research was funded by Italian Ministry of University and Research, grant number PRIN 20227K7YJS.

## CRediT authorship contribution statement

**Ilenia Grieco:** Writing – original draft, Validation, Investigation, Formal analysis, Data curation. **Davide Bassani:** Writing – original draft, Validation, Investigation, Formal analysis, Data curation. **Letizia Trevisan:** Writing – original draft, Data curation. **Veronica Salmasso:** Writing – review & editing, Supervision, Methodology. **Eleonora Cescon:** Data curation. **Filippo Prencipe:** Investigation. **Tatiana Da Ros:** Writing – review & editing. **Loreto Martinez-Gonzalez:** Writing – original draft, Data curation. **Ana Martinez:** Methodology. **Giampiero Spalluto:** Methodology, Funding acquisition, Conceptualization. **Stefano Moro:** Methodology, Funding acquisition. **Stephanie Federico:** Writing – review & editing, Supervision, Project administration, Methodology, Funding acquisition, Conceptualization.

## Declaration of competing interest

The authors declare that they have no known competing financial interests or personal relationships that could have appeared to influence the work reported in this paper.

## Appendix A. Supplementary data

Supplementary data to this article can be found online at <https://doi.org/10.1016/j.bioorg.2024.107659>.

## References

- [1] L.J. Fulcher, G.P. Sapkota, Functions and regulation of the serine/threonine protein kinase CK1 family: Moving beyond promiscuity, *Biochem. J* 477 (2020) 4603–4621, <https://doi.org/10.1042/BCJ20200506>.
- [2] Knippschild U, Krüger M, Richter J, Xu P, Balbina García-Reyes, Peifer C, et al. The CK1 family: Contribution to cellular stress response and its role in carcinogenesis. *Front Oncol* 2014;4 MAY. <https://doi.org/10.3389/fonc.2014.00096>.
- [3] L.H. Rosenberg, J.L. Cleveland, W.R. Roush, D.R. Duckett, CK1 $\delta$ : an exploitable vulnerability in breast cancer, *Ann Transl Med* 4 (2016) 474. <https://doi.org/10.21037/ATM.2016.12.15>.
- [4] E.L. Mazzoldi, A. Pastò, E. Ceppelli, G. Pilotto, V. Barbieri, A. Amadori, et al., Casein Kinase 1 Delta Regulates Cell Proliferation, Response to Chemotherapy and Migration in Human Ovarian Cancer Cells. *Front. Oncol* (2019) 9, <https://doi.org/10.3389/fonc.2019.01211>.
- [5] J.-P. Etchegaray, K.K. Machida, E. Noton, C.M. Constance, R. Dallmann, N.M.N. Di, et al., Casein Kinase 1 Delta Regulates the Pace of the Mammalian Circadian Clock, *Mol. Cell Biol.* 29 (2009) 3853–3866, <https://doi.org/10.1128/MCB.00338-09>.
- [6] D. Dorin-Semblat, C. Demarta-Gatsi, R. Hamelin, F. Armand, T.G. Carvalho, M. Moniatte, et al., Malaria Parasite-Infected Erythrocytes Secrete PfCK1, the Plasmodium Homologue of the Pleiotropic Protein Kinase Casein Kinase 1, *PLoS One* 10 (2015) e0139591.

- [7] E. Durieu, E. Prina, O. Leclercq, N. Oumata, N. Gaboriaud-Kolar, K. Vougiopoulou, et al., From drug screening to target deconvolution: A target-based drug discovery pipeline using *Leishmania* casein kinase 1 isoform 2 to identify compounds with antileishmanial activity, *Antimicrob. Agents Chemother.* 60 (2016) 2822–2833, <https://doi.org/10.1128/AAC.00021-16>.
- [8] D. Catarzi, F. Varano, E. Viganini, C. Lambertucci, A. Spinaci, R. Volpini, et al., Casein Kinase 1 $\delta$  Inhibitors as Promising Therapeutic Agents for Neurodegenerative Disorders, *Curr. Med. Chem.* 29 (2022) 4698–4737, <https://doi.org/10.2174/0929867329666220301115124>.
- [9] G. Li, H. Yin, J. Kuret, Casein Kinase 1 Delta Phosphorylates Tau and Disrupts Its Binding to Microtubules, *J. Biol. Chem.* 279 (2004) 15938–15945, <https://doi.org/10.1074/JBC.M314116200>.
- [10] Chen C, Gu J, Basurto-Islas G, Jin N, Wu F, Gong CX, et al. Up-regulation of casein kinase 1 $\epsilon$  is involved in tau pathogenesis in Alzheimer's disease. *Scientific Reports* 2017 7:1 2017;7:1–15. <https://doi.org/10.1038/s41598-017-13791-5>.
- [11] F. Kametani, T. Nonaka, T. Suzuki, T. Arai, N. Dohmae, H. Akiyama, et al., Identification of casein kinase-1 phosphorylation sites on TDP-43, *Biochem. Biophys. Res. Commun.* 382 (2009) 405–409, <https://doi.org/10.1016/j.bbrc.2009.03.038>.
- [12] Okochi M, Walter J, Koyama A, Nakajo S, Baba M, Iwatsubo T, et al. Constitutive Phosphorylation of the Parkinson's Disease Associated-Synuclein\*. 2000.
- [13] T. Nonaka, G. Suzuki, Y. Tanaka, F. Kametani, S. Hirai, H. Okado, et al., Phosphorylation of TAR DNA-binding protein of 43 kDa (TDP-43) by truncated casein kinase 1 $\delta$  triggers mislocalization and accumulation of TDP-43, *J. Biol. Chem.* 291 (2016) 5473–5483, <https://doi.org/10.1074/jbc.M115.695379>.
- [14] L. Badura, T. Swanson, W. Adamowicz, J. Adams, J. Cianfrogna, K. Fisher, et al., An inhibitor of casein kinase 1 $\epsilon$  induces phase delays in circadian rhythms under free-running and entrained conditions, *J. Pharmacol. Exp. Ther.* 322 (2007) 730–738, <https://doi.org/10.1124/jpet.107.122846>.
- [15] Q.J. Meng, E.S. Maywood, D.A. Bechtold, W.Q. Lu, J. Li, J.E. Gibbs, et al., Entrainment of disrupted circadian behavior through inhibition of casein kinase 1 (CK1) enzymes, *PNAS* 107 (2010) 15240–15245, <https://doi.org/10.1073/pnas.1005101107>.
- [16] P. Adler, J. Mayne, K. Walker, Z. Ning, D. Figeys, Therapeutic Targeting of Casein Kinase 1 $\epsilon$  in an Alzheimer's Disease Mouse Model, *J. Proteome Res.* 18 (2019) 3383–3393, <https://doi.org/10.1021/acs.jproteome.9b00312>.
- [17] S. Mente, E. Arnold, T. Butler, S. Chakrapani, R. Chandrasekaran, K. Cherry, et al., Ligand-protein interactions of selective casein kinase 1 $\delta$  inhibitors, *J. Med. Chem.* 56 (2013) 6819–6828, <https://doi.org/10.1021/jm4006324>.
- [18] M. Bibian, R.J. Rahaim, J.Y. Choi, Y. Noguchi, S. Schürer, W. Chen, et al., Development of highly selective casein kinase 1 $\delta$ /1 $\epsilon$  (CK1 $\delta/\epsilon$ ) inhibitors with potent antiproliferative properties, *Bioorg. Med. Chem. Lett.* 23 (2013) 4374–4380, <https://doi.org/10.1016/j.bmcl.2013.05.075>.
- [19] N. Oumata, K. Bettayeb, Y. Ferandin, L. Demange, A. Lopez-Giral, M.L. Goddard, et al., Roscovitine-derived, dual-specificity inhibitors of cyclin-dependent kinases and casein kinases 1, *J. Med. Chem.* 51 (2008) 5229–5242, <https://doi.org/10.1021/jm800109e>.
- [20] I.G. Salado, M. Redondo, M.L. Bello, C. Perez, N.F. Liachko, B.C. Kraemer, et al., Protein kinase CK-1 inhibitors as new potential drugs for amyotrophic lateral sclerosis, *J. Med. Chem.* 57 (2014) 2755–2772, <https://doi.org/10.1021/jm500065f>.
- [21] E.P. Cuevas, L. Martinez-Gonzalez, C. Gordillo, C. Tosat-Bitrián, C. Pérez de la Lastra, A. Sáenz, et al., Casein kinase 1 inhibitor avoids TDP-43 pathology propagation in a patient-derived cellular model of amyotrophic lateral sclerosis, *Neurobiol. Dis.* 192 (2024) 106430, <https://doi.org/10.1016/j.nbd.2024.106430>.
- [22] I. Grieco, M. Bissaro, D.B. Tiz, D.I. Perez, C. Perez, A. Martinez, et al., Developing novel classes of protein kinase CK1 $\delta$  inhibitors by fusing [1,2,4]triazole with different bicyclic heteroaromatic systems, *Eur. J. Med. Chem.* 216 (2021) 113331, <https://doi.org/10.1016/j.ejmech.2021.113331>.
- [23] Caulkett PWR, Jones G, MM, Renshaw ND, Stewart SK,, Wright B. caulkett1995. J Chem Soc n.d.
- [24] Matasi, 2006 n.d.
- [25] O. Piša, S. Rádl, Synthesis of 4-Quinolones: N, O-Bis(trimethylsilyl)acetamide-Mediated Cyclization with Cleavage of Aromatic C-O Bond, *European J Org Chem* 2016 (2016) 2336–2350, <https://doi.org/10.1002/ejoc.201600178>.
- [26] Hutton, 1994 n.d.
- [27] S. Redenti, I. Marcovich, T. De Vita, C. Pérez, R. De Zorzi, N. Demitri, et al., A Triazolotriazine-Based Dual GSK-3 $\beta$ /CK-1 $\delta$  Ligand as a Potential Neuroprotective Agent Presenting Two Different Mechanisms of Enzymatic Inhibition, *ChemMedChem* 14 (2019) 310–314, <https://doi.org/10.1002/cmdc.201800778>.
- [28] D. Sabbadin, S. Moro, Supervised molecular dynamics (SuMD) as a helpful tool to depict GPCR-ligand recognition pathway in a nanosecond time scale, *J. Chem. Inf. Model.* 54 (2014) 372–376, <https://doi.org/10.1021/ci400766b>.
- [29] M. Pavan, G. Bolcato, D. Bassani, M. Sturlese, S. Moro, Supervised Molecular Dynamics (SuMD) Insights into the mechanism of action of SARS-CoV-2 main protease inhibitor PF-07321332, *J. Enzyme Inhib. Med. Chem.* 2021 (36) (2021) 1646–1650, <https://doi.org/10.1080/14756366.2021.1954919>.
- [30] G. Bolcato, M. Pavan, D. Bassani, M. Sturlese, S. Moro, Ribose and Non-Ribose A2A Adenosine Receptor Agonists: Do They Share the Same Receptor Recognition Mechanism? *Biomedicines* (2022) 10, <https://doi.org/10.3390/biomedicines10020515>.
- [31] G. Bolcato, E. Cescon, M. Pavan, M. Bissaro, D. Bassani, S. Federico, et al., Article a computational workflow for the identification of novel fragments acting as inhibitors of the activity of protein kinase ck1 $\delta$ , *Int. J. Mol. Sci.* (2021) 22, <https://doi.org/10.3390/ijms22189741>.
- [32] H. Alonso, A.A. Bliznyuk, J.E. Gready, Combining docking and molecular dynamic simulations in drug design, *Med. Res. Rev.* 26 (2006) 531–568, <https://doi.org/10.1002/med.20067>.
- [33] G. Rastelli, L. Pinzi, Refinement and rescoring of virtual screening results, *Front. Chem.* (2019) 7, <https://doi.org/10.3389/fchem.2019.00498>.
- [34] L. Di, E.H. Kerns, K. Fan, O.J. McConnell, G.T. Carter, High throughput artificial membrane permeability assay for blood-brain barrier, *Eur. J. Med. Chem.* 38 (2003) 223–232, [https://doi.org/10.1016/S0223-5234\(03\)00012-6](https://doi.org/10.1016/S0223-5234(03)00012-6).
- [35] M.V. Berridge, A.S. Tan, Characterization of the Cellular Reduction of 3-(4,5-dimethylthiazol-2-yl)-2,5-diphenyltetrazolium bromide (MTT): Subcellular Localization, Substrate Dependence, and Involvement of Mitochondrial Electron Transport in MTT Reduction, *Arch. Biochem. Biophys.* 303 (1993) 474–482, <https://doi.org/10.1006/abbi.1993.1311>.
- [36] Y. Iguchi, M. Katsuno, S. Takagi, S. Ishigaki, J. Niwa, M. Hasegawa, et al., Oxidative stress induced by glutathione depletion reproduces pathological modifications of TDP-43 linked to TDP-43 proteinopathies, *Neurobiol. Dis.* 45 (2012) 862.
- [37] M. Pavan, S. Menin, D. Bassani, M. Sturlese, S. Moro, Implementing a Scoring Function Based on Interaction Fingerprint for Autogrow4: Protein Kinase CK1 $\delta$  as a Case Study, *Front. Mol. Biosci.* (2022) 9.
- [38] H.M. Berman, J. Westbrook, Z. Feng, G. Gilliland, T.N. Bhat, H. Weissig, et al., The Protein Data Bank, *Nucleic Acids Res.* 28 (2000) 235–242, <https://doi.org/10.1093/nar/28.1.235>.
- [39] Molecular Operating Environment (MOE), 2019.01; Chemical Computing Group ULC, 1010 Sherbooke St. West, Suite #910, Montreal, QC, Canada, H3A 2R7, 2021. n.d.
- [40] D. Case, T. Darden, T. Cheatham, C. Simmerling, J. Wang, R. Duke, et al., *AMBER 10*, University of California, San Francisco, 2008.
- [41] QUACPAC 2.2.3.3. OpenEye, Cadence Molecular Sciences, Santa Fe, NM. <http://www.eyesopen.com>. n.d.
- [42] Korb O, Stützel T, Exner TE. LNCS 4150 - PLANTS: Application of Ant Colony Optimization to Structure-Based Drug Design. n.d.
- [43] W.L. Jorgensen, J. Chandrasekhar, J.D. Madura, R.W. Impey, M.L. Klein, Comparison of simple potential functions for simulating liquid water, *J. Chem. Phys.* 79 (1983) 926–935, <https://doi.org/10.1063/1.445869>.
- [44] A. Bakan, L.M. Meireles, I. Bahar, ProDy: Protein Dynamics Inferred from Theory and Experiments, *Bioinformatics* 27 (2011) 1575–1577, <https://doi.org/10.1093/BIOINFORMATICS/BTR168>.
- [45] J.C. Phillips, D.J. Hardy, J.D.C. Maia, J.E. Stone, J.V. Ribeiro, R.C. Bernardi, et al., Scalable molecular dynamics on CPU and GPU architectures with NAMD, *J. Chem. Phys.* 153 (2020) 44130, [https://doi.org/10.1063/5.0014475/16709547/044130\\_1\\_ACCEPTED\\_MANUSCRIPT.PDF](https://doi.org/10.1063/5.0014475/16709547/044130_1_ACCEPTED_MANUSCRIPT.PDF).